MODELLING OF PULLOUT RESISTANCE OF CONCRETE ANCHOR BLOCK EMBEDDED IN COHESIONLESS SOIL

by

Rowshon Jadid

A thesis submitted to the Department of Civil Engineering, Bangladesh University of Engineering and Technology, Dhaka, in partial fulfilment of the degree of Master of Science in Civil and Geotechnical Engineering**.**

DEPARTMENT OF CIVIL ENGINEERING
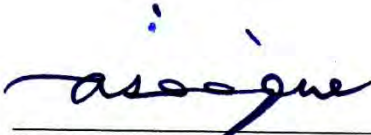
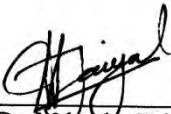BANGLADESH UNIVERSITY OF ENGINEERING AND TECHNOLOGY

May, 2016

The thesis titled "**Modelling of Pullout Resistance of Concrete Anchor Block Embedded in Cohesionless Soil**", submitted by **Rowshon Jadid**, Student number- **0413042239 P** and session **April, 2013** has been accepted as satisfactory in partial fulfilment of the requirement for the degree of Master of Science (Civil and Geotechnical Engineering) on **28 May, 2016**.

Board of Examiners

(1)

Dr. Md. Zoynul Abedin
Professor
Department of Civil Engineering
BUET, Dhaka-1000

Chairman
(Supervisor)

(2)

Dr. Abdul Muqtadir
Professor and Head
Department of Civil Engineering
BUET, Dhaka-1000

Member
(Ex-officio)

(3)

Dr. Abu Siddique
Professor
Department of Civil Engineering
BUET, Dhaka-1000

Member

(4)

Dr. Md. Abu Taiyab
Professor
Department of Civil Engineering
DUET, Gazipur.

Member
(External)

DECLARATION

I certify that, although I have conferred with others in preparing this thesis and drawn upon a range of sources cited in this work, the content and concept of this thesis is my original work. Neither the thesis nor any part has been submitted to or is being submitted elsewhere for any other purposes.

Rowshon Jadid

TABLE OF CONTENTS

LIST OF FIGURES

LIST OF TABLES

NOTATION

B	Height of anchor block
E_b	Modulus of elasticity of concrete anchor block
E_{OED}	Initial stiffness of soil
E_{ur}	Unloading/reloading stiffness of soil
E_{50}	Secant stiffness of soil
FE	Finite element
H	Depth of embedment of anchor block
H/B	Embedment depth ratio of anchor block
HS	Hardening soil model
K_4	Failure point at load-displacement curve
L	Length of anchor block
L/B	Aspect ratio of anchor block
P_u	Ultimate pullout capacity of anchor block
m	Power for stiffness stress dependency
MC	Mohr-Coulomb model
$MAPE$	Mean Absolute Percentage Error
N	Break-out factor
R_{inter}	Interface reduction factor
t	Thickness of anchor block
α	angle of side flanks of the wedge
β	angle of Rankine passive failure surface with the vertical face of block
δ_t	angle of friction between soil and top surface of the block
δ_b	angle of friction between soil and bottom surface of the block
δ_s	angle of friction between soil and side surface of the block

ACKNOWLEDGEMENT

ABSTRACT

Anchor block is a specially designed concrete member intended to withstand pullout or thrust forces from backfill material of an anchored earth retaining wall by passive resistance of soil in front of the block. Present study describes the theoretical and numerical investigations into the behaviour of an anchor block in cohesionless soil. While analysing theoretically, a passive wedge of soil was assumed to develop in front of the anchor block due to the pullout force exerted from retaining wall via rebar. The equilibrium condition of the wedge was employed to propose a new analytical method to estimate the pullout capacity of an anchor block embedded in shallow depth. The comparison of the proposed theoretical predictions with the existing theoretical and experimental studies shows that, the proposed method provides a better estimate of the pullout capacity. Furthermore, the theoretical results are facilitated with charts which may be used in hand calculations to obtain an estimate of anchor capacity for most frequently used shapes, cube and square with half of height/length of block as thickness. The use of these charts is illustrated by worked examples.

Finite Element (FE) analysis was also conducted using PLAXIS to investigate the effect of anchor shape, embedment depth and ground water table on pullout resistance of anchor block. The effect of anchor shape was found to be considerable for small aspect ratio of anchor block, whereas the influence of ground water table was substantial only when the ground water table was located anywhere between the ground surface and the base of the anchor block. Based on numerical analysis, an empirical correlation was developed to determine the correction factor that accounts the effect of ground water table. The proposed analytical method showed very close agreement with FE analysis for shallow embedment depth of anchor block. In addition, the failure modes of the soil body were also observed. These findings may be useful to all those dealing with civil engineering projects and research works on anchored retaining earth wall.

CHAPTER 1
INTRODUCTION

1.1   General

In many instances, the design of civil engineering structures requires that the foundation systems withstand the horizontal pullout forces. In such circumstances, an efficient and economic design solution may be obtained through the use of tension members. These tension members, which are denoted as earth anchors, are typically attached with the retaining structure and embedded in the soil to sufficient depth so that they can resist pullout forces with safety. They are generally used to transmit tensile forces from a structure to the foundation soil thus generating passive support to structures like bulkheads, sheet piles and retaining walls. Their pullout capacity is obtained considering shear strength and dead weight of the surrounding soil mass. The use such anchors in retaining structure may reduce the construction cost as much as 43 to 64% (Khan and Sikder, 2004). However, inadequate anchorage systems constitute most of the causes of failure of sheet-pile walls (Daniel and Olson, 1982; Sowers and Sowers, 1973). Various types of anchor include anchor plates and beams (deadman), tie backs, anchor plates, anchor beams supported by batter piles, and block anchors. According to Bowles (1997), block anchors are cast-in-place or precast concrete members as shown in Figure 1.1, that may be square or rectangular in section with necessary length to develop adequate passive resistance. Anchor block can be installed by excavating the ground to the required depth, placing the anchor, and then backfilling with soil. When used as a support for retaining structures, anchors are installed in excavated trenches and connected to tie rods that may be driven or placed through augered holes. This type of anchor is of interest in the present study.

1.2   Background and Present State of the Problem

In Bangladesh, two anchored earth walls have been implemented; one in Kalyanpur, Dhaka and the other in BCIC industrial area, Narayanganj for establishing a substation for Dhaka Electric Supply Authority (DESA) in 2002 and 2003 respectively, where anchored systems were designed according to the guidelines provided by BS 8006 (1995). This code states

that the ultimate pullout resistance of an anchor block is four times the passive pressure force acting on anchor block (ignoring the insignificant amount of resistance offered by rebar). Recently, Mostopha (2013) conducted extensive laboratory tests to investigate the pullout capacity of concrete anchor block located at different horizontal distances from yielding boundary wall. He found that the maximum resisting force of concrete anchor block is always less than four times the Rankine's passive thrust acting on the anchor block, and recommended to use the passive resistance coefficient less than 4 to ensure safe design. Although no unsatisfactory performance has been reported from those projects, an arbitrarily chosen higher factor of safety was used while designing to ensure safety (Mostofa, 2013).
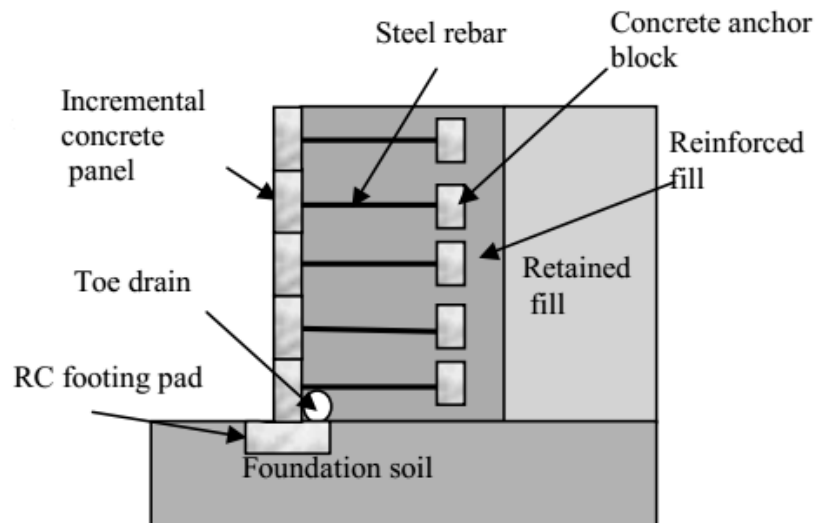
Figure 1.1 Anchored retaining earth wall (Khan and Sikder, 2004)

Literature reveals that many researches have been conducted on the capacity of vertical anchors especially for anchor plate including that by Hueckel (1957), Ovesen and Stromann (1972), Neely, et al. (1973), Das (1975), Akinmusuru (1978), and Ghaly (1997) etc. However, only few studies were found for block anchor, Bowles (1997), Duncan and Mokwa (2001), Naser (2006) and Mostofa (2013).

Bowles's (1997) calculated passive earth resistance against anchor blocks using conventional lateral earth pressure theories, and is applicable for long and continuous wall structure. According to Ovesen (1964), the passive earth pressure against short structures (e.g. anchor block) is higher than those predicted by conventional theories, and the difference can be quite significant. Thus, Bowles's (1997) model yields lower value than

2

the actual pullout capacity of anchor block. Duncan and Mokwa (2001), Naser (2006) and Mostofa (2013) conducted experimental studies on anchor block.

It is clear that the majority of past research has been experimentally based and, as a result, current design practices are largely based on empiricism. In contrast, very few thorough theoretical and numerical analyses have been performed to determine the ultimate pullout loads of anchor block. Of the numerical studies that have been presented in the literature, few can be considered as rigorous. In addition, hardly any researches were conducted on the effect of ground water table.

To address these issues, this research work aims to propose a new theoretical approach to calculate the ultimate pullout capacity of an anchor block embedded in cohesionless soil. A finite element analysis will be conducted using PLAXIS software to substantiate the proposed theoretical method. Moreover, an effort will be taken to make comparison between different geotechnical models that can be used to design anchor block. The comparison is useful, because in the daily practice of geotechnical engineering many discussions arise on which model is most suitable in which situation. This is also mainly due to the differences in results between different models. Sharp designs can reduce cost massively.

1.3   Objective of the Research

The present study aims to achieve the following objectives:

i.   To propose a new theoretical method which can be used to predict the ultimate pullout capacity of anchor block embedded in cohesionless soil.

ii.   Finite element analysis using PLAXIS software to investigate the effect of anchor shape, embedment depth and ground water table on pullout resistance of anchor block.

iii. To make comparison between different geotechnical models with laboratory/field tests, so that suitable method or methods with greater accuracy and computationally ease can be adopted for different conditions.

1.4   Organization of the Thesis

The thesis consists of five chapters. Chapter 1 is an introduction that includes the problem statement and objective of this study along with the thesis organization. Chapter 2 presents the literature review including the experimental, theoretical and numerical studies

conducted on anchor block and plate etc. Chapter 3 introduces the derivation of theoretical approach to calculate the pullout capacity of anchor block. The proposed theoretical approach is also compared with the existing theoretical and experimental studies. Chapter 4 presents the numerical analyses on anchor block, which mainly focuses on the effect of anchor shape, embedment depth and ground water table on pullout resistance. Additionally, different constitutive models are compared to assess their suitability at different state of affairs. The main conclusions drawn from the theoretical and numerical analyses are presented in Chapter 5, along with the recommendations for future work.

CHAPTER 2
LITERATURE REVIEW

2.1   General

In order to provide a satisfactory background of subsequent discussions, a summary of research into vertical anchor plate/block behaviour is presented. A comprehensive overview on the topic of anchors is given by Das (1990). Although the research work aims to focus on the analysis of concrete anchor block in cohesionless soil, emphasis on vertical anchor plate will be equally given, because most of the time anchor block is designed using the principle of vertical anchor plate (Das, 2007). Research into the behaviour of soil anchors can take one of three forms, namely experimental-based, theoretical-based and numerical–based studies. The brief summary of existing research herein has been separated based on this distinction. No attempt is made to present a complete bibliography of all research; rather a more selective overall summary of research with greatest relevance to the current study is presented. In addition, contributions made to the behaviour of circular, multiple underreamed, or multihelix anchors have not been reviewed.

2.2   Previous Experimental Investigations

Although there are no entirely adequate substitutes for full-scale field testing, tests at the laboratory scale have the advantage of allowing close control of at least some of the variables encountered in practice. In this way, trends and behaviour patterns observed in the laboratory can be of value in developing an understanding of performance at larger scales. In addition, observations made in laboratory testing can be used in conjunction with mathematical analyses to develop semi-empirical theories. These theories can then be applied to solve a wider range of problems. In this section, a brief discussion will be presented on anchor plate. Whereas the experimental studies on anchor block will be discussed elaborately in a separate subsection, since the results of these studies will be utilised in the subsequent chapters.

2.2.1 Anchor plate

Experimental investigations on plate anchor behaviour have generally adopted one of the two approaches, namely, conventional methods under "normal gravity" conditions or centrifuge systems. Both the methods have advantages and disadvantages, and these must be borne in mind when interpreting the results from experimental studies of anchor behaviour. Numerous investigators have performed model tests in an attempt to develop semi-empirical relationships that can be used to estimate the capacity of anchor plates in cohesionless soil. This is evidenced by the number of studies shown in Table 2.1. Illustrations of notation used in this table are presented in Figure 2.1.

The works prior to 1970 have not been presented in Table 2.1. This includes the field and (or) model testing of vertical square and rectangular anchors by Hueckel (1957), Smith (1962), Smith et.al. (1965) etc. In the majority of these earlier studies, a failure mechanism was assumed and the pullout capacity was then determined by considering the equilibrium of the soil mass around the anchor and contained by the assumed failure surface.

| (a) | (b) |
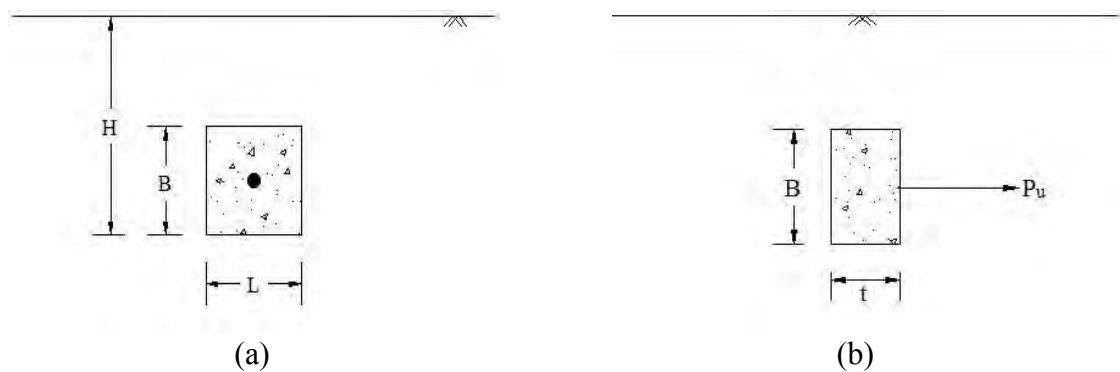
Figure 2.1 Problem notation (a) Front view, (b) Side view of an anchor

2.2.2 Anchor block

In contrast of previous researches on anchor plates, only few experimental studies were found for anchor block, Duncan and Mokwa (2001), Naser (2006) and Mostopha (2013). Table 2.2 summarizes the experimental studies conducted on anchor block. Duncan and Mokwa (2001) carried out passive pressure load tests at the Virginia Tech field test site at Kentland Farms near Blacksburg.

Table 2.1 Laboratory model tests and field tests on vertical anchor plate in cohesionless soil (Modified from Merifield and Sloan, 2006)

Source	Type of testing	Anchor shape	Anchor size (mm)	Friction angle (°)	Anchor roughness (°)	H/B
Neely et. al. (1973)	Chamber	Square; rectangular	50.8	38.5	21	1–5
Das (1975)	Chamber	Square; circular	38–76	34	?	1–5
Akinmusuru (1978)	Chamber	Strip; rectangular; square; circular; L/B = 2,50 10		24; 35	?	1–10
Ovesen (1981)	Centrifuge; field	Square	20	29.5–37.7	?	1–3.39
Rowe and Devis (1982)	Sand Chamber	Square; rectangular; L/B = 1–8.75	51	32	?	1-8
Dickin and Leung (1983, 1985)	Centrifuge chamber	Square; rectangular; strip	25; 50	41[a]	Polished, 29	1–8; 1–13
Hoshiya and Mandal (1984)	Sand chamber	Square; rectangular; L/B = 2, 4, 6	25.4	29.5	?	1–6
Murray and Geddes (1989)	Sand chamber	Square; rectangular; L/B = 1–10	50.8	43.6, dense	10.6	1–8
Dickin and King (1997)	Centrifuge	Rectangular; L/B = 7.8	25	37.3-46.1	?	1-12

[a]Mobilized plane strain friction angle, φ'_{mp}

Table 2.2 Laboratory model tests and field test on vertical anchor block in cohesionless soil

Source	Type of testing	Anchor Block shape	Anchor Block size (mm)	Friction angle (°)	Anchor roughness (°)	H/B
Duncan and Mokwa (2001)	Field	Rectangular; L/B = 1.7	1100 x 1900 x 900	50	6	1
Naser (2006)	Chamber	Square	150 x 150 x 150	43.5	7.3-11.2	2
Mostofa (2013)	Chamber	Square	150 x 150 x 75	37.2- 44.8	?	3.2

The tests were performed using the test arrangements shown in Figure 2.2. Using a pile group for reaction, horizontal loads were applied to a concrete anchor block 3.5-ft high, 6.3-ft long, and 3.0-ft thick (1100 x 1900 x 900 mm). Figure 2.3 shows comparisons of measured and computed load-deflection curves, using the log spiral value of P_u corrected for 3D effects proposed by Ovesen (1964).
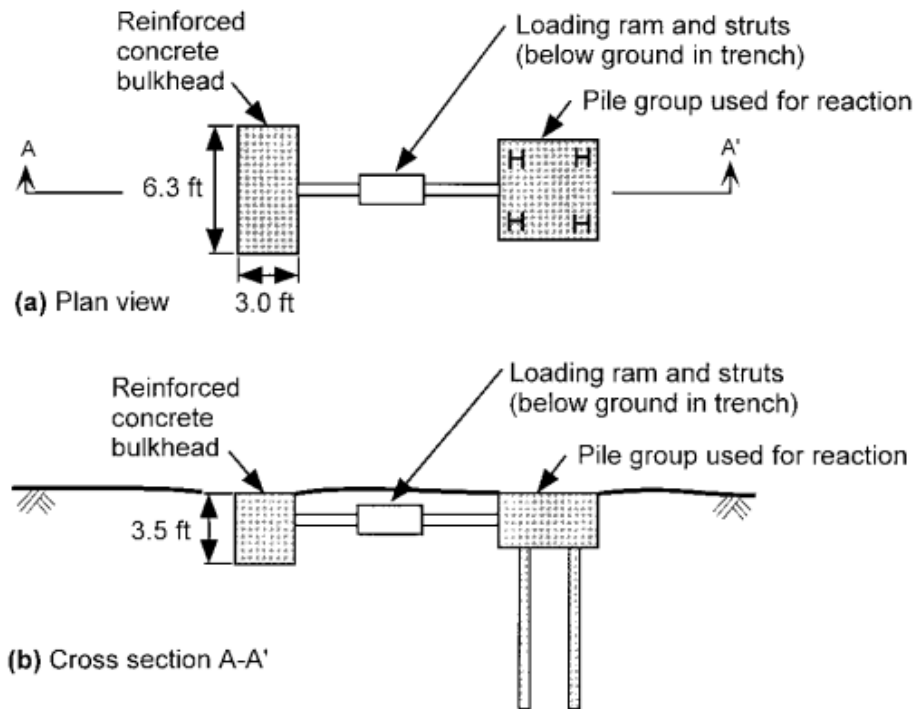
Figure 2.2 Test arrangement for passive pressure load tests (Duncan and Mokwa, 2001)
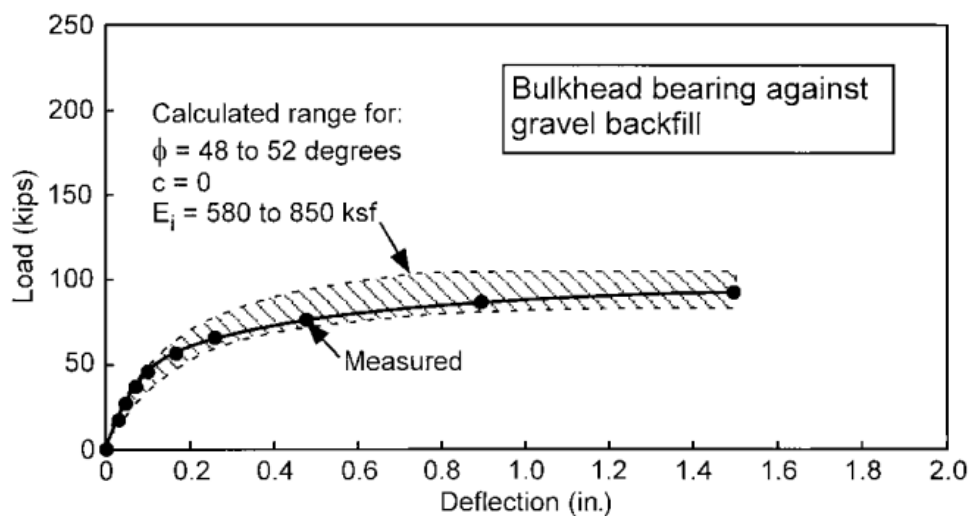
Figure 2.3 Computed and measured load-deflection curves for passive pressure load tests (Duncan and Mokwa, 2001)

8

Naser (2006) performed laboratory pullout tests on 150 × 150 × 150 mm concrete block anchors embedded in sand at a depth of 300 mm. The sand was deposited in a chamber of dimensions 1200 × 800 × 600 mm using a pluviation method to ensure a uniform and reproducible density. He compared the experimental results with the analytical calculations by Rankine, Coulomb, and log spiral theories. Figure 2.4 shows typical the load-displacement relationship for block anchor embedded in sand at dry, wet and saturated conditions.
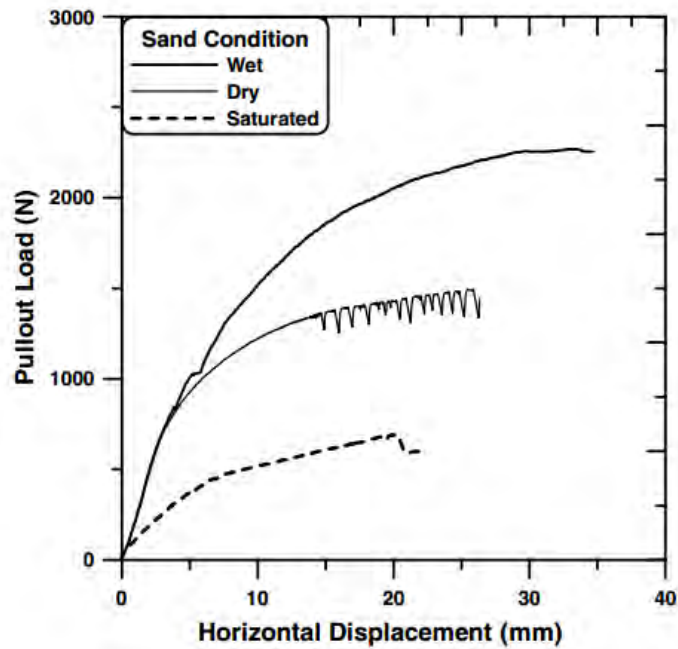
Figure 2.4 Load-displacement curves for anchor block in sand of different moisture conditions (Naser, 2006)

Mostofa (2013) investigated the pullout capacity of concrete anchor block located at different distances from yielding boundary wall and embedded in air dry sand, using small scale laboratory experimental works. The experimental setup consisted of a large tank made of fibre glass sheets and steel framing system. A series of tests was carried out in the tank to investigate the load-displacement behaviour of anchor block. Figure 2.5 shows the variation of ultimate resistance with angle of internal friction of soil. He also proposed the passive resistance coefficient which should be multiplied with the passive resistance in front of the anchor block to obtain the pullout capacity of anchor block.

More specific details of these studies will be provided in the later chapters of this thesis, when several previous theoretical studies are compared with the new theoretical approach proposed in the current study.
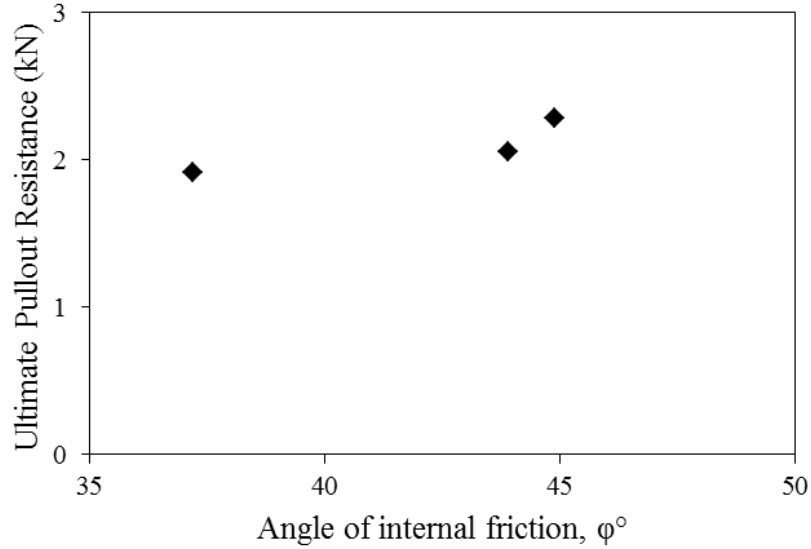
Figure 2.5 Variation of ultimate pullout resistance with angle of internal friction of soil (Mostofa, 2013)

2.3   Previous Theoretical Investigation

The previous theoretical studies post-1970 for vertical anchors, which are commonly used by practicing engineers, will be discussed elaborately in this section. As mentioned earlier, the theoretical methods of calculating pullout capacity of vertical anchor plate are commonly employed for anchor block also (Das, 2007). Thus, no effort has been made here to distinguish between anchor plate and anchor block design method. Previous theoretical studies of anchors in sand have typically utilized simple analytical approaches such as limiting equilibrium, cavity expansion, and limit analysis.   In the limit equilibrium method, a failure surface is assumed along with a distribution of stress along that surface. Equilibrium conditions are then considered for the failing soil mass, and an estimate of the collapse load is obtained.

2.3.1 Ovesen and Stromann (1972)

Ovesen and Stromann (1972) proposed a semi-empirical method for determining the ultimate resistance of anchors in sand. When an anchor slab has a height of B, equal to the depth of embedment H and is continuous (Figure 2.6), the ultimate resistance per unit length of anchor, P_u' can be calculated from Eq. (2.1).

$$P_u' = \frac{1}{2} \ H^2 (K_p \cos \ ' - K_a \cos \varphi')$$ (2.1)

10
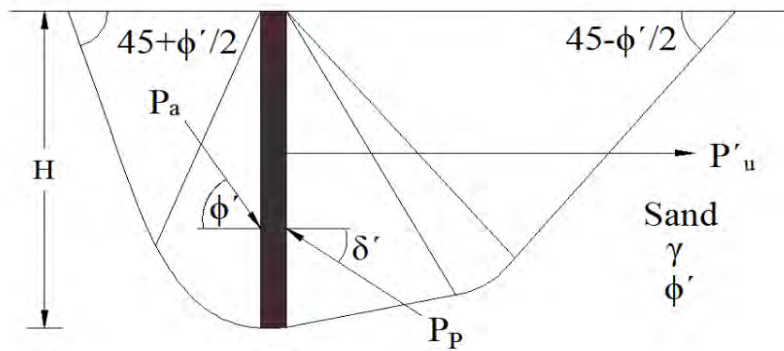
Figure 2.6 Basic case continuous vertical anchor in granular soil (Das, 2007)

Where δ' is the friction angle between anchor slab and soil, K_a is the active earth pressure coefficient with $\delta'=\varphi'$, and K_p is the passive earth pressure coefficient. The term $K_p \cos \delta'$ of Eq. (2.1) can be obtained from Figure 2.7 using the value of $K_p \sin \delta' = (W + 0.5 \gamma H^2 K_a \sin \varphi')/(0.5 \gamma H^2)$ and the angle of internal friction φ'. Where W is the effective weight per unit length of anchor slab.
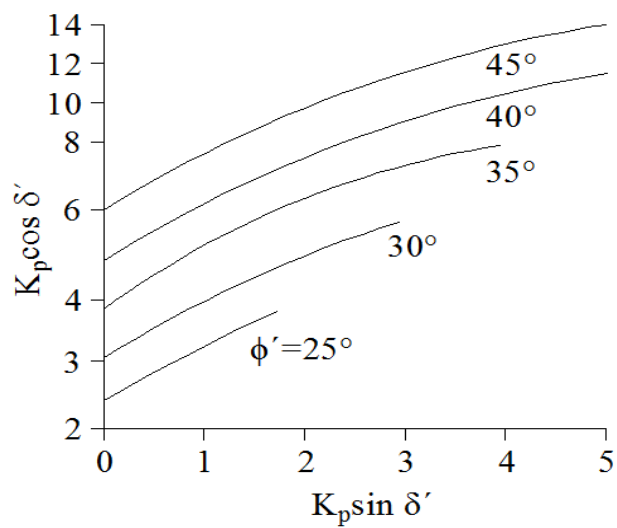
Figure 2.7 Variation of $K_p \cos \delta'$ with $K_p \sin \delta'$ (Ovesen and Stromann, 1972)
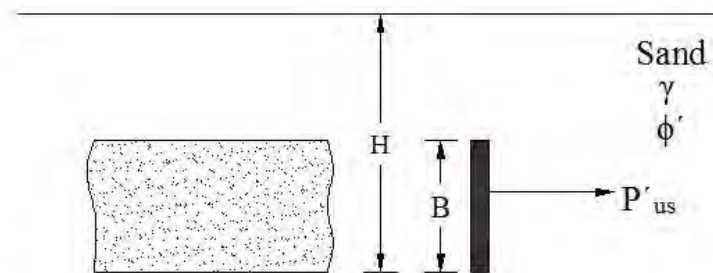
Figure 2.8 Strip case vertical anchor (Das, 2007)

11

For a continuous strip anchor (Figure 2.8) of height B (which is less than the depth of embedment, H), the ultimate resistance per unit length is corrected as:

$$P'_{us} = \left[\frac{C_{ov} + 1}{C_{ov} + \frac{H}{B}}\right] P'_u \qquad (2.2)$$

Where P'_{us} is the ultimate resistance for strip case, $C_{ov}= 19$ for dense sand and 14 for loose sand. In practice, the anchor plates are placed in a row with center-to-center spacing S'(Figure 2.9). The ultimate resistance of each anchor of length L is

$$P_u = P'_{us}L_e \qquad (2.3)$$

Where, L_e is the equivalent length and can be obtained from Figure 2.10.
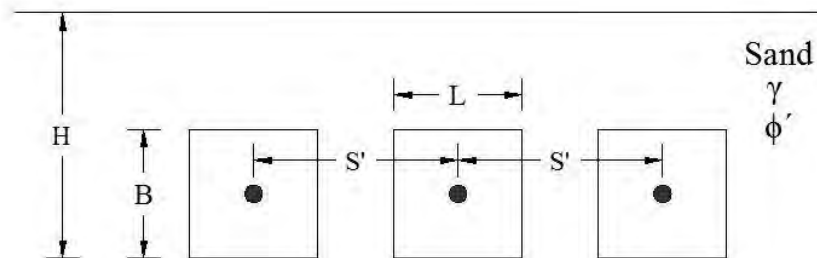
Figure 2.9 Actual case for row anchors (Das, 2007)
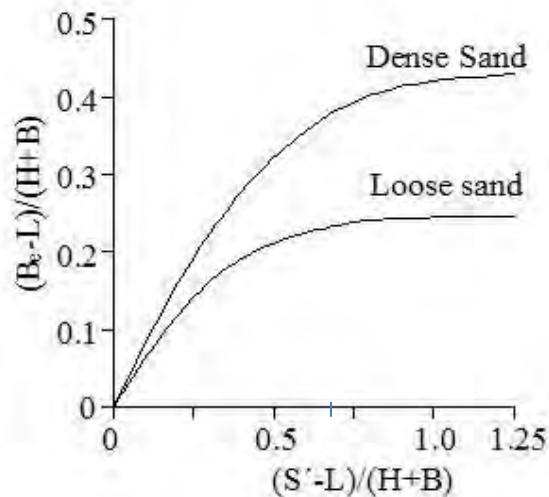
Figure 2.10 Variation of $(B_e - L)/(H + B)$ with $(S' - L)/(H + B)$ (Ovesen and Stromann, 1972)

12

2.3.2 NAVFAC DM 7.02 (U.S. Navy, 1986)

A step-by-step design procedure of vertical anchors can be found in the design manual of Naval Facilities Engineering Command (NAVFAC DM 7.02, 1986) by U.S. Navy. According to NAVFAC DM 7.02 (1986), the anchor blocks should be placed outside the surface making an angle equal to angle of friction of backfill soil, φ with the horizontal as shown in Figure 2.11. The anchor blocks locating between φ line and Rankine's failure surface will generate partial passive resistance. Design of anchor blocks using active and passive earth pressures in accordance with the NAVFC DM 7.02 (1986) are briefly illustrated in Figure 2.12 and Figure 2.13. A factor of safety 2 against pullout resistance is suggested in this method.
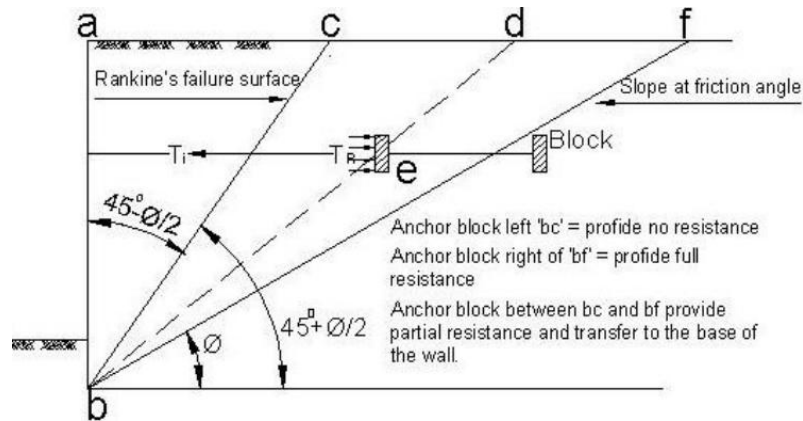
Figure 2.11 Effect of anchor location relative to the wall (adapted from NAVFAC DM 7.02, 1986)
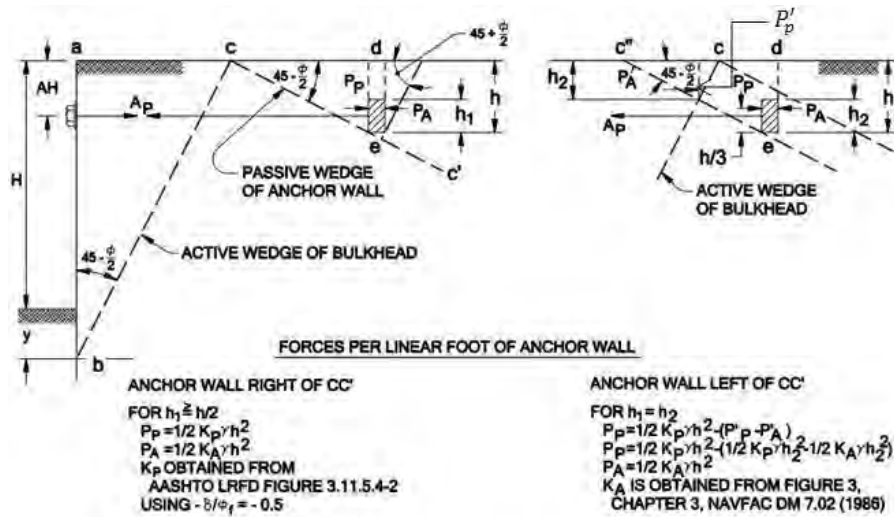
Figure 2.12 Active and passive earth pressure calculation for continuous anchor wall located between rupture surface and slope at friction angle (adapted from NAVFAC DM 7.02, 1986)

13

ANCHORAGE RESISTANCE FOR $h_1 \geq \frac{h}{2}$

1. CONTINUOUS WALL:
   ULTIMATE $A_{pc}/d = P_P - P_A$ WHERE A_{pc}/d IS ANCHOR RESISTANCE AND P_P, P_A TAKEN PER LINEAL FOOT OF WALL.
2. INDIVIDUAL ANCHORS:
   IF $d > b + h$, ULTIMATE $A_p = b(P_P - P_A) + 2P_0$ TAN ϕ, WHERE P_0 = RESULTANT FORCE OF SOIL AT REST ON VERTICAL AREA cde OR C'' de.
   IF $d = h+b$, A_p/d IS 70% OF A_{pc}/d FOR CONTINUOUS WALL.
   L FOR THIS CONDITION IS L' AND L' = h.
   IF $d < h + b$, $A_p/d + A_{pc}/d = A_{pc}/d - \frac{L'}{L}(0.3 A_{pc}/d)$, L' = h.

ANCHOR RESISTANCE FOR $h_1 < \frac{h}{2}$
   ULTIMATE A_p/d OR A_{pc}/d EQUALS BEARING CAPACITY OF STRIP FOOTING OF WIDTH h_1 AND SURCHARGE LOAD $\gamma(h - \frac{h_1}{2})$, SEE FIGURE 1, CHAPTER 4, NAVFAC DM 7.02 (1986)
   USE FRICTION ANGLE ϕ': WHERE TANϕ' = 0.6 TANϕ.

Figure 2.13 Design criteria for deadman anchorage (adapted from NAVFAC DM 7.02, 1986)

2.3.3 BS 8006 (British Standard, 1995)

BS 8006 (1995) recommends to use passive resistance coefficient while caculating the pullout resistance of an anchor block. This is based on the fact that, the conditions at the ends of the structures are quite different from those at the centre, which has significant influence on the passive resistance. Ovesen (1964) found that the passive earth pressure against short structures is higher than those predicted by conventional theories (Rankine and Coulomb theories), and the difference can be quite significant. Hansen (1966) developed a method for correcting the results of conventional pressure theories for shape (or 3-D) effects. For short anchors, the ultimate resistance should be multiplied by a coefficient (M) to account for 3-D effects. For a plate anchor passive resistance coefficient (M) is given as:

$$M = 1 + \left(K_p - K_a\right)^{0.67}\left[1.1E^4 + \frac{1.6F}{1 + 5\left(\frac{L}{B}\right)} + \frac{0.4\left(K_p - K_a\right)E^3F^2}{1 + 0.05\left(\frac{L}{B}\right)}\right] \qquad (2.4)$$

Where, K_p and K_a are the coefficients of passive and active earth pressure respectively, E = 1-B/H and $F = 1 - (L/S')^2$, and S' is the center-to-center distance between two anchors. The anchor block geometry used in Eq. (2.4) can be found in Figure 2.1. The above equation considers both the embedment factor (E) and the shape factor (F). The value of F is 0.0 for long and continuous anchor, and is 1.0 for single short anchor. According to the BS 8006 (1995) and Jones (1996), the horizontal pullout resistance of an

14

anchor block is 4 times the passive pressure force acting on anchor block (ignoring the insignificant amount of resistance offered by rebar) i.e. passive resistance coefficient, $M = 4$ is suggested. A factor of safety 2.5 to 3 is used in this method. However, the experimental studies by Mostofa (2013) indicated that this coefficient is always less than 4.

2.3.4 Ghaly (1997)

Ghaly (1997) used the results of 104 laboratory tests, 15 centrifugal tests, and 9 field tests to propose an empirical correlation for the ultimate resistance of single anchors, where unit weight and internal friction angle of soil ranged from 14 to16 kN/m^3 and 34° to 38.5^o respectively. The embedment depth ratio (H/B) of the anchor plate varied between 1 and 4. This data was incorporated in a generalized from to predict the ultimate horizontal pullout resistance of anchor plates in terms of the influencing parameters. The correlation can be expressed as:

$$P_u = \frac{5.4}{tan\, \varphi'} \left(\frac{H^2}{A} \right)^{0.28} AH \tag{2.5}$$

Where A is the area of the anchor $= BL$.

2.3.5 Bowles (1997)

Based on horizontal equilibrium analysis of lateral earth pressures and frictional resistances acting on an anchor block as depicted in Figure 2.14, Bowles (1997) proposed a general equation to determine the horizontal pullout resistance of anchor as follows:

$$P_u = L\left(P_p' - P_a' + F_{top} + F_{bot} \right) \tag{2.6}$$

Where P_p' and P_a' are the passive and active thrust acting on the anchor block respectively, and the frictional resistances (F_{top} and F_{bot}) can be determined when the angle of friction between soil and concrete (δ and δ_1) acting at the top and bottom of the anchor block as shown in Figure 2.14 is known. For maximum efficiency, Bowles (1997) suggested to locate the anchor block such that the Rankine passive zone in front of the anchor block should be completely outside the Rankine active zone behind the retaining wall. A factor of safety 1.2 to 1.5 is suggested for this method.
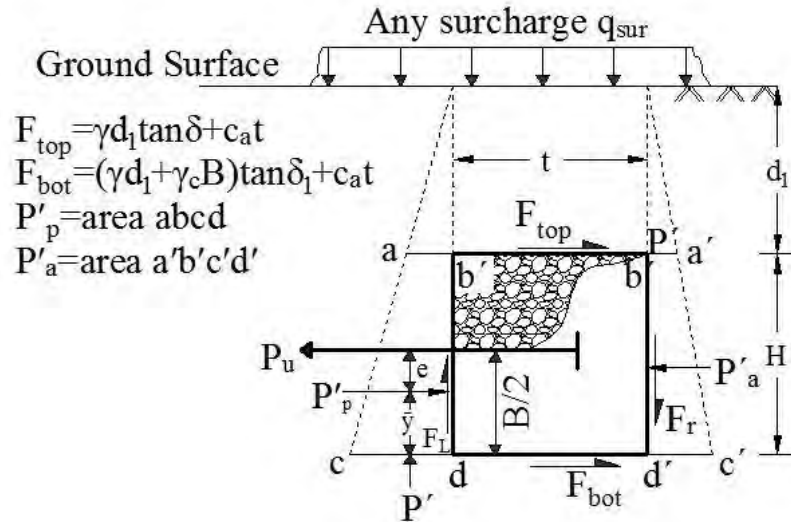
Figure 2.14 Complete set of forces, not including q_{sur}, acting on any anchor block
(Bowles, 1997)
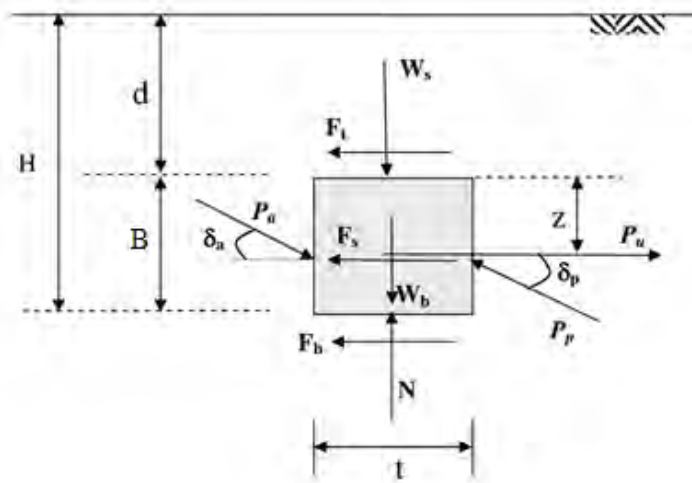
Figure 2.15 Free body diagram of anchor block (Naser, 2006)

2.3.6 Naser (2006)

Naser (2006) analysed pullout capacity of an anchor block using limit equilibrium approach (Figure 2.15). The ultimate pullout capacity of block anchor block (P_u) was obtained from the equilibrium of forces acting on the block by summing them along the horizontal direction and multiplying the lateral earth pressures (passive and active) by the 3-D correction factor M, to yield the following equation.

$$P_u = M\left(P_{p,h} - P_{a,h}\right) + F_t + F_s + F_b \qquad (2.7)$$

Where, F_t, F_b and F_s are the effective friction forces at the top, bottom and at two side of the block, $P_{p,h}$ is the effective horizontal passive thrust and $P_{a,h}$ is the effective horizontal active thrust. The 3-D correction factor (M) may be calculated from Eq.(2.4). He found that the pullout capacity of block anchor with Rankine's theory (1857), corrected for the 3-D effect with the contribution of friction showed a close agreement with experimental results.

2.4   Previous Numerical Investigations

Although there are a variety of experimental results in the literature, very few rigorous numerical analyses have been performed to determine the pullout capacity of anchors in sand (Merifield and Sloan, 2006). Most of those numerical analyses were performed for strip anchor. On the other hand, to the knowledge of the author, hardly any effort has been made so far to conduct numerical analysis on anchor block. Although it is essential to verify theoretical solutions with experimental studies wherever possible, results obtained from laboratory testing alone are typically problem specific. Since the cost of performing laboratory tests on each and every field problem combination is prohibitive, it is necessary to be able to model soil pullout resistance numerically for the purposes of design. A summary of some important previous numerical studies post-1980 on vertical anchors is provided in Table 2.3.

Table 2.3 Numerical studies on vertical anchors in cohesionless soil (Modified from Merifield and Sloan, 2006)

Source	Analysis method	Anchor shape	Anchor roughness	Friction angle (°)	H/B
Rowe and Davis (1982)	Elastoplastic finite element	Strip	Smooth	0–45	1–8
Hanna et al. (1988)	Limiting equilibrium	Strip; inclined	?	All	All
Murray and Geddes (1989)	Limit analysis – upper bound	Strip; inclined	Smooth; rough	43.6	1–8
Basudhar and Singh (1994)	Limit analysis – lower bound	Strip	Rough; smooth	32; 35; 38	1–5
Merifield and Sloan (2006)	Limit analysis – upper and lower bound	Strip	Rough	20-40	1-10

The most complete numerical study first appears to be that by Rowe and Davis (1982). They described a theoretical assessment of anchor plates in sand which considered the effect of anchor plate embedment, friction angle, dilatancy, and initial stress state and anchor plate roughness for vertical anchor plates. Their theoretical solution was based on an elasto-plastic finite element analysis using a soil structure interaction theory. The sand was assumed to have a Mohr-Coulomb failure criterion. The theoretical data were presented in the form of design charts which could be used in hand calculations to obtain an estimate of anchor plate capacity for a wide range of anchor plate geometries and sand. The failure pattern and zones of plastic yielding obtained from their numerical analysis is shown in Figure 2.16. The finite element method has also been used by Vemeer and Sutjiadi (1985), Tagaya et al. (1983, 1988) and Koutsabeloulis and Griffiths (1989), and Sakai and Tanaka (1998) for horizontal anchor plates. However, limited results of these studies were presented in literature.
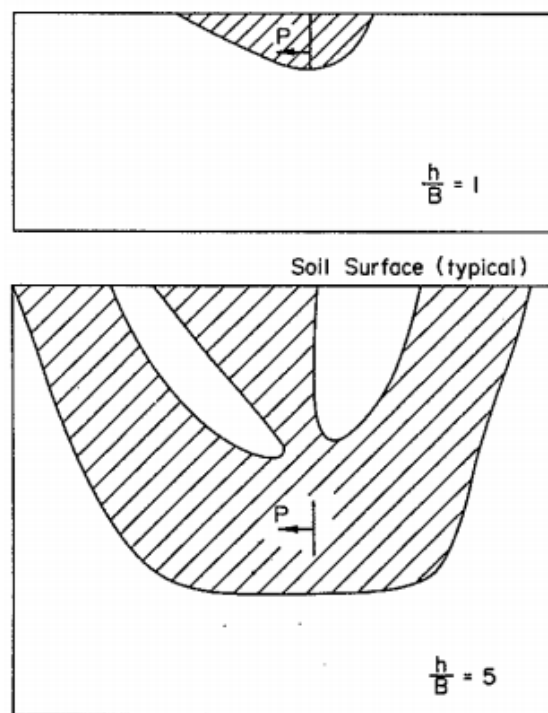
Figure 2.16 Failure pattern and zones of plastic yielding for rough anchor plates by Rowe and Davis (1982)

Tagaya et. al. (1983, 1988) conducted two dimensional plane strain and axisymmetric finite element analyses by the constitutive law of Lade and Duncan (1975). Scale effects for circular anchor plates in dense sand were investigated by Sakai and Tanaka (1998) by a constitutive model for a non-associated strain hardening-softening elasto-plastic material.

18

Koutsabeloulis and Griffiths (1989) investigated the trap door problem by the initial stress finite element method. Both plane strain and axisymmetric works were conducted. The researchers concluded that an associated flow rule has little effect on the collapse load for strip anchor plates but a significant effect (30%) for circular anchor plates. Large displacements were observed for circular anchor plates prior to collapse.

Upper and lower bound limit analysis techniques have been used by Murray and Geddes (1987, 1989) and Basudhar and Singh (1994) to estimate the capacity of vertical strip anchor plates. Basudhar and Singh (1994) obtained estimates with a generalized lower bound procedure based on finite element method and non-linear programming similar to that of Sloan (1988). The solutions of Murray and Geddes (1987, 1989) were obtained by typically constructing kinematic ally admissible failure mechanisms (upper bound).

Merifield et al. (2006) presented the results of a rigorous numerical work to estimate the ultimate capacity load for vertical anchor plate in cohesionless material. Rigorous bounds have been obtained using two numerical procedures that are based on finite element method of the upper and lower bound of limit analysis. For comparison purposes, numerical and theoretical results of the break-out factor have also been obtained by the more conventional displacement finite element method. Results are presented in the familiar form of break-out factors based on various soil strength profiles and geometries and are compared with existing numerical and empirical solutions. The failure pattern and zones of plastic yielding obtained from their numerical analysis is shown in Figure 2.17.

$H/B = 5$, $\phi' = 30°$, $\gamma H/c' = 100$
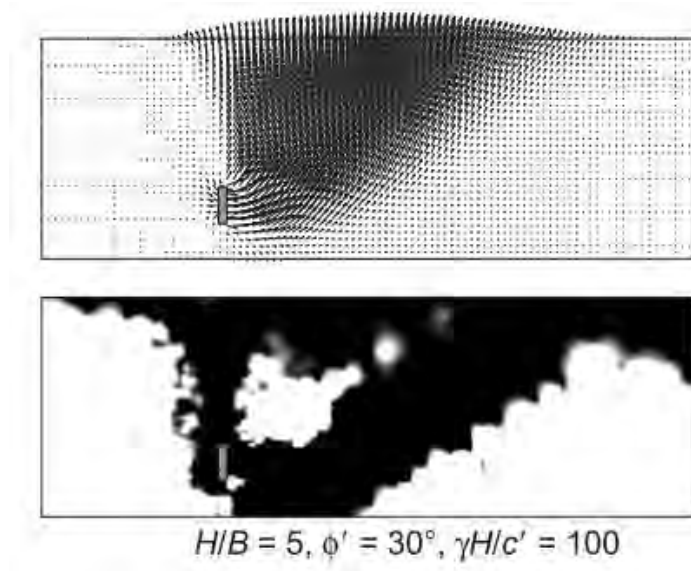
Figure 2.17 Failure pattern and zones of plastic yielding for rough anchor plates by
Merifield and Sloan (2006)

2.5   Factors Affecting the Pullout Capacity

The ultimate pullout capacity of an anchor block depends on several factors. Some of the most important governing factors are-

(i)   Embedment depth ratio (H/B),

(ii)   Aspect ratio or length-to- height ratio (L/B)

(iii) Shear strength parameters of the soil (soil friction angle, φ and cohesion, C); and

(iv)   The angle of friction at the anchor-soil interface, δ
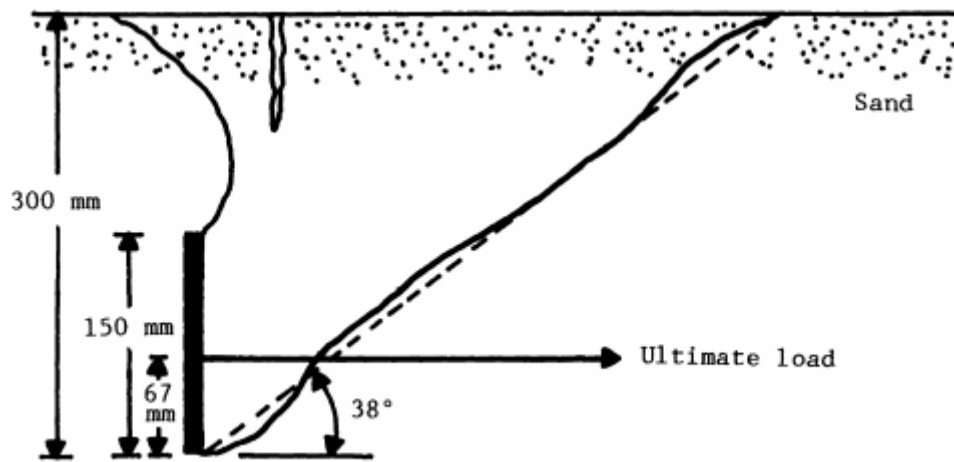
Figure 2.18 Failure surface in front of a square anchor slab (150 mm x 150 mm) embedded in sand at $H/B = 2$ as observed by Hueckel (1957)

The pullout capacity of an anchor is primarily derived from the passive force imposed by the soil in front of the anchor slab. If the embedment depth ratio (H/B) of the anchor is relatively small, at ultimate pullout load on the anchor the passive failure surface developed in soil in front of the anchor will intersect the ground surface. This is referred to as shallow anchor condition. Figure 2.18 shows the failure surface in front of a shallow square plate anchor (that is, $H=2B$) embedded in sand as observed by Hueckel (1957). At greater embedment ratios, the local shear failure in soil will take place at ultimate load, and these anchors are called deep anchor (Das, 1990). The aspect ratio also affects the pullout capacity of an anchor. If the aspect ratio of an anchor is large enough, the anchor can be considered as strip anchor. Two-dimensional plane strain case is applicable for strip anchor. However, for square anchor three-dimensional analysis is required as the boundary conditions at the ends of failure surface is quite different than the strip anchor. The numerical studies by Rowe and Davis (1982) and Merifield and Sloan (2006) show that

20

the interface roughness has a significant effect on pullout capacity of strip anchor. Changing the interface roughness from perfectly rough to perfectly smooth can lead to a reduction in the anchor capacity by as much as 65% (Merifield and Sloan, 2006). More specific details of these factors will be discussed in the later chapters of this thesis.

2.6   Concluding Remarks

Literature review reveals that most of past research has been carried out experimentally and, as a result, current design practices are largely based on empiricism. Consequently, the results obtained from these empirical methods are generally case specific. Thus, a generalized analytical approach is required to resolve this problem. Reported literature on the effect of ground water table on pullout capacity are also very few. This is another important design consideration that needs to be addressed. Although, many geotechnical models are available regarding the design of vertical anchors, with today's most used models, comparisons between the models and measurements are very rare. The comparison is useful as because in practice of geotechnical engineering many discussions arise on which model is most suitable in which situation. This is also mainly due to the differences in results between different models. This thesis, as such, is intended to make a contribution to the design of anchored retaining earth wall by conducting an extensive investigation on these issues.

CHAPTER 3

THEORITICAL ANALYSIS OF ANCHOR BLOCK

3.1   General

From literature review, it is quite evident that many researches have been conducted on the capacity of vertical anchors especially with anchor plate. However, studies on anchor block are limited compared to the anchor plate (Naser, 2006). The theoretical methods of calculating pullout capacity of vertical anchor plate are commonly employed for anchor block also (Das, 2007). On the contrary, this study shows the limitations of these methods while using them to calculate the pullout resistance of anchor block. Consequently, an effort has been taken to propose an analytical method to calculate the pullout capacity of anchor block, which is presented in the first part of the chapter. Later, the predictions of the proposed method are compared with the laboratory and field test results available in the literature along with other methods to assess the suitability of these methods.

3.2   Principle of the Proposed Method

In this method, a passive wedge model is employed to derive analytical expression to calculate the ultimate pullout capacity of anchor block in cohesionless soil. The passive-wedge model is based on the principle that normal stresses will increase in front of the anchor block due to the pullout force exerted from retaining wall via rebar. The increasing stresses cause the soil to move up, and a passive wedge will develop as schematized in Figure 3.1. It is assumed that the resistance of the soil will be provided by the normal force acting perpendicular to the bottom of the failure plane and the friction forces along the side planes of the failure wedge. The normal force, self-weight of failure wedge and the friction forces acting on the wedge can be determined from geometry of the wedge and properties of the soil. Thus, the ultimate resistance of the soil (P_u) then can be derived from the equilibrium of the wedge. Passive wedge model was successfully used for the analysis of anchor plate by Dickin and Leung (1985), for the analysis of laterally loaded pile by Gabr and Borden (1990), Mirzoyan (2007) and Cheng et. al. (2014).

The proposed method is restricted to shallow laid anchor block in cohesionless soil. For shallow anchors, the embedment ratio is such that, failure surface reaches the ground

surface at limit equilibrium; whereas for deep anchors, the embedment ratio is such that, failure surface does not reach the ground surface at limit equilibrium (Das, 1990).
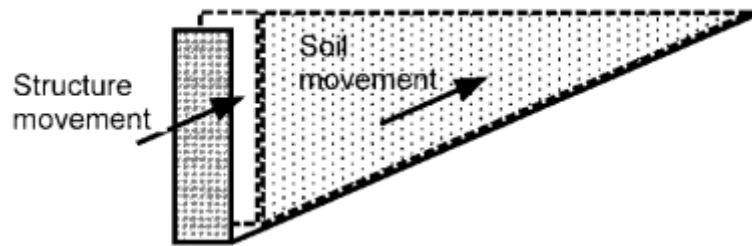
Figure 3.1 Structure and soil movement on the verge of pullout failure of an anchor block (Duncan and Mokwa, 2001)

3.2.1 Geometry of the failure surface

The assumed failure surfaces in the proposed method and the forces acting in the failure mechanism are illustrated in Figure 3.2. Three assumptions are made on the geometry of failure surface.

(i)   The passive failure surface in front of the anchor block is planer and reaching up to the top level of anchor block. Zone *ABC* in Figure 3.2(a) is considered as a Rankine passive zone.

(ii) The soil located above the top of the anchor is a simple surcharge, $q = \gamma(H - B)$.

(iii) Failure planes around anchor radiate outwards. Thus, the soil wedge has an extension with two side flanks, which have an angle α as shown in Figure 3.2(b).

The first assumption was made for the simplicity of the analysis, although the actual failure surface follows very irregular pattern and reaches up to the ground surface for shallow anchor. The second assumption neglected the shearing resistance of soil above the top of the anchor block, but the effect of soil weight above the base is considered by superimposing an equivalent surcharge. Neely et. al. (1973) also neglected shearing resistance of soil above anchor for the analysis of pullout resistance of strip anchor, while Tarzaghi (1948) neglected soil resistance above footing level for the analysis of bearing capacity of soil. Soil resistance of cohesionless soil is generally calculated from peak angle of internal friction φ_p, that is obtained from plain strain shear tests or triaxial tests. However, the failure of the soil mass is rather progressive, and the applicable value of φ is

moblized friction angle (φ_m), which is generally less than the peak value (Dickin and Leung, 1985; Das, 1990). Therefore, neglecting shear resistance above anchor level, somewhat balance the overestimation of pullout capacity due to the use of φ_p obtained from test results. The third assumption was made from soil's dilatancy property.
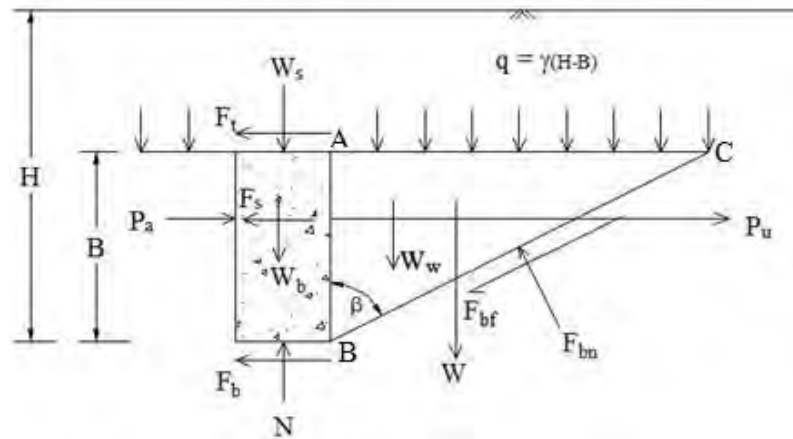
(a)
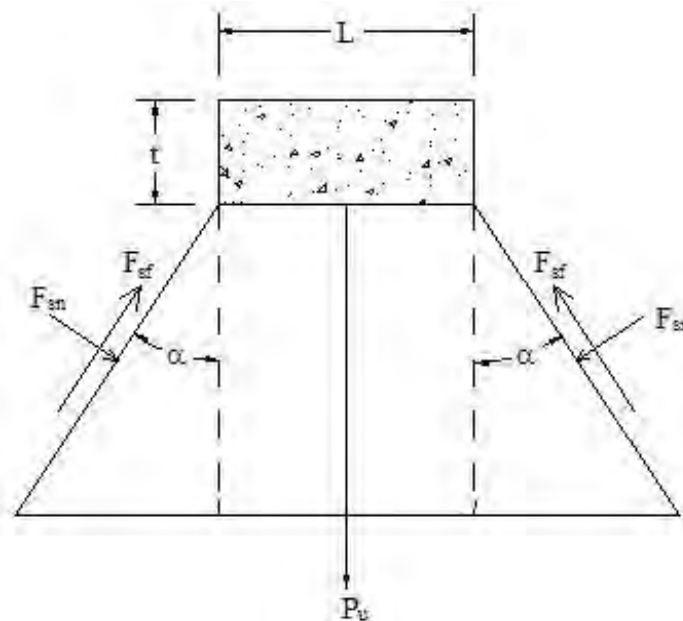
(b)

Figure 3.2 Idealized failure zone in front of single anchor with acting forces.
(a) Elevation, (b) Plan section of an anchor block

Many soils (e.g. dense sand) dilate during plastic deformation and this charachteistic of the soil may have a significant effect on anchor behaviour. Dilatancy during plastic

24

deformation tends to cause the soil in front of the anchor to lock up and it is necessary for an extensive plastic region to develop before there is sufficient freedom for collapse to occur (Rowe and Davis, 1982). Laboratory test reults and numerical analysis also confirmed the formation of side wedges caused by dilation of soil (Rowe and Davis, 1982; Dickin and Leung, 1983). As an approximation Reese, Cox, and Koop (1974) suggested to use $\alpha = \varphi/2$, where, φ is the angle of internal friction of soil. Mirzoyan (2007) conducted field tests on laterally loaded pile and found that α is about 75% of the angle of internal friction.

3.2.2 Forces acting on anchor block

Figure 3.2 shows the elevation and plan section of a short anchor block embedded in sand, with all forces acting on it and with friction considered. For an anchor block with the dimensions height (B), width (L), thickness (t) and the depth of embedment below soil surface (H); the acting forces are as follows:

$$
\begin{aligned}
F_{bn} &= \text{normal force at the bottom of the wedge} \\
F_{bf} &= \text{friction force at the bottom of the wedge} \\
F_{sn} &= \text{normal force at the side of the wedge} \\
F_{sf} &= \text{friction force at the side of the wedge} \\
N &= \text{normal force at the bottom of the anchor block} \\
F_b &= \text{friction force at the bottom of the block} \\
F_t &= \text{friction force at the top of the block} \\
F_s &= \text{friction force at two sides of the block} \\
P_a &= \text{resultant active thrust} \\
W_w &= \text{weight of the wedge} \\
W_q &= \text{weight of the surcharge above wedge} \\
W_b &= \text{weight of the block anchor} \\
W_s &= \text{weight of soil above the block anchor} \\
W &= \text{total weight of the block-wedge system} \\
&= W_w + W_q + W_b + W_s
\end{aligned}
$$

3.2.3 Friction between soil and structure

Anchor blocks are relatively light structure and are not supported by rigid structures. The upward components of the passive resistance is large enough to cause upward movement of the anchor block, and the soil and structure move together as illustrated in Figure 3.1 (Duncan and Mokwa, 2001). Thus, the weight of the anchor block and the weight of soil above it should be considered for the vertical equilibrium of wedge (Duncan and Mokwa, 2001; Naser, 2006). Shear displacement between soil and structure is not expected to occur in the vertical direction of plane AB, Figure 3.2 (a); accordingly, interface friction is neglected along this direction. However, frictional resistance between soil and structure develops in the horizontal direction, e.g. F_t, F_b, F_s in Figure 3.2 (a), since the pullout force from retaining wall causes horizontal shear displacement between soil and anchor block.

The magnitude of this type of resistance depends on the angle of friction between soil and structure, δ. The maximum possible value of δ depends on the roughness of the interface and properties of the soil. It is convenient to characterize values of δ_{max} in terms of the ratio δ_{max}/φ, where φ is the angle of internal friction of soil. The value of δ_{max}/φ varies between 0 and 1 depending upon surface roughness, mean particle size of sand and method of installation (CFEM, 2006; Tiwari, et al., 2010). Potyondy (1961) conducted interface shear tests on a variety of structural materials and soils and found smallest value of δ_{max}/φ = 0.76 for concrete. As an approximation, Singh (1967) suggested following values (1) δ_{max}/φ = 1/3 for smooth structure (wall), (2) δ_{max}/φ = 2/3 for ordinary retaining wall, (3) δ_{max}/φ = 3/4 for rough walls with well-drained backfill, and (4) $\delta = 0$ when backfill is subjected to vibrations. The range of values of δ between fine sand and concrete is 15-25$^{\rm o}$, Das (1995) and Bowles (1997); whereas Naser (2006) found the value of δ_{max} as 38$^{\rm o}$. More recently, Gireesha and Muthukkumaran (2011); Tiwari and Al-Adhadh (2014) conducted numerous laboratory tests to study soil-structure frictional resistance, and observed that δ_{max}/φ varies between 0.76-0.79 and 0.69-0.94 respectively between concrete and sand depending upon the relative density and degree of saturation of soil.

Some amount of relative shear displacement across the interface is required to mobilize interface friction. The amount of relative shear displacement required to mobilize the full strength of the interface is not large, typically not more than 0.1 – 0.25 in. (2.5 – 6 mm). Smaller relative displacements across the interface will result in only partial mobilization

of the interface friction. Therefore, δ_{mob} will be less than or equal to δ_{max} (Duncan and Mokwa, 2001).

In other circumstances, the heavy anchor block (e.g. strip anchor) moves horizontally while the soil moves both horizontally and upward. As a result of the upward movement of the soil with respect to the structure, there is an upward shear force on the structure and a downward shear force on the soil. In the case of a rough anchor, significant shear stresses will develop at the anchor interface in response to this upward movement. These shear stresses are resisted by the interface and contribute significantly to the anchor capacity (Merifield and Sloan, 2006; Kame, et al., 2012).
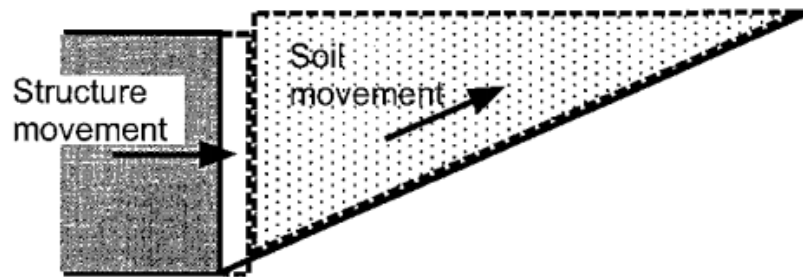
Figure 3.3 Structure and soil movements for heavy anchor block (Duncan and Mokwa, 2001)

3.3   Proposed Analysis for Anchor Block Capacity

3.3.1 Computation of soil reaction at the bottom of the wedge

The ultimate pullout capacity of block anchor (P_u) can be obtained from the equilibrium of forces acting on the block and wedge illustrated in Figure 3.2. First, we will consider the vertical equilibrium of the block and wedge to determine the normal force at the bottom of the wedge (F_{bn}).

Thus, Force equilibrium in the vertical direction:

$$\sum F_V = W + 2F_{sf}cos\beta - F_{bn}sin\beta + F_{bf}cos\beta = 0 \qquad (3.1)$$

Substituting $F_{bf} = F_{bn}tan\varphi'$ into Eq. (3.1):

$$W + 2F_{sf}cos\beta - F_{bn}sin\beta + F_{bn}tan\varphi'\,cos\beta = 0 \qquad (3.2)$$

Solving Eq. (3.2) for F_{bn}:

$$F_{bn} = \frac{W + 2F_{sf}cos\beta}{sin\beta - tan\varphi'cos\beta} \qquad (3.3)$$

3.3.2 Computation of pullout capacity of anchor block

Force equilibrium in the horizontal direction:

$$\sum F_H = P_u - 2F_{sf}\sin\beta\cos\alpha + 2F_{sn}\sin\alpha - F_{bn}\cos\beta - F_{bf}\sin\beta + P_a$$
$$- F_b - F_s - F_t = 0 \tag{3.4}$$

Substituting $F_{bf} = F_{bn}\tan\varphi'$ into Eq. (3.4):

$$P_u - 2F_{sf}\sin\beta\cos\alpha + 2F_{sn}\sin\alpha - F_{bn}\cos\beta - F_{bn}\tan\varphi'\sin\beta + P_a$$
$$- F_b - F_s - F_t = 0 \tag{3.5}$$

Rearranging the Eq. (3.5) for ultimate pullout capacity of anchor block (P_u):

$$P_u = 2F_{sf}\sin\beta\cos\alpha - 2F_{sn}\sin\alpha + F_{bn}\cos\beta + F_{bn}\tan\alpha\sin\beta - P_a$$
$$+ F_b + F_s + F_t \tag{3.6}$$

Now, substituting the value of F_{bn} from Eq. (3.3) into Eq. (3.6):

$$P_u = 2F_{sf}\sin\beta\cos\alpha - 2F_{sn}\sin\alpha + \frac{(W + 2F_{sf}\cos\beta)(\cos\beta + \tan\varphi'\sin\beta)}{\sin\beta - \tan\varphi'\cos\beta}$$
$$- P_a + F_b + F_s + F_t \tag{3.7}$$

After simplification:

$$P_u = 2F_{sf}\sin\beta\cos\alpha - 2F_{sn}\sin\alpha + \frac{(W + 2F_{sf}\cos\beta)}{\tan(\beta - \varphi')} - P_a + F_b + F_s + F_t \tag{3.8}$$

Where,

$$\frac{\cos\beta + \tan\varphi'\sin\beta}{\sin\beta - \tan\varphi'\cos\beta} = \frac{1 + \sin\beta\tan\varphi'}{\tan\beta - \tan\varphi'} = \frac{1}{\tan(\beta - \varphi')} \tag{3.9}$$

Naser (2006) observed that, anchor thickness contributed to the pullout capacity through friction forces. This contribution was not significant as compared to the passive resistance. Jones (1996) also reported that the passive resistance has the greatest influence on pullout capacity of anchor block, and it derives from the passive wedge in front of the anchor. Thus, neglecting frictional forces and active thrust from Eq. (3.8), one may obtain simplified and computationally easy form of Eq. (3.8) as follow:

$$P_u = \frac{W}{\tan(\beta - \varphi')} \tag{3.10}$$

The accuracy and the applicability of Eq. (3.8) and Eq. (3.10) will be discussed in the later sections of this chapter.
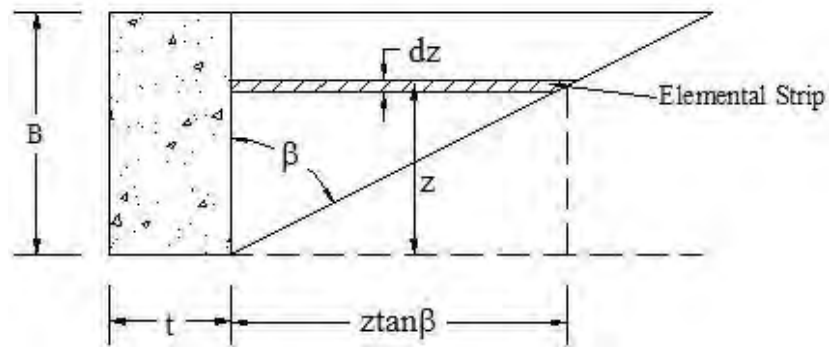
(a)
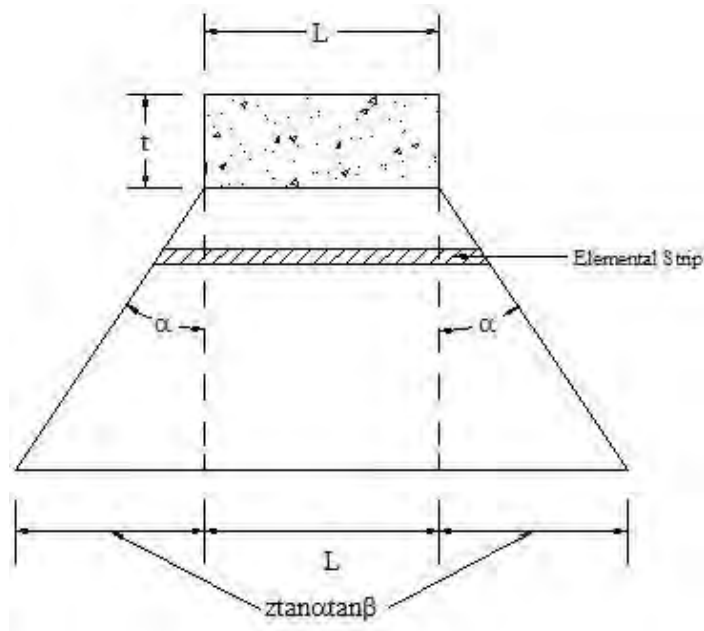
(b)

Figure 3.4 Determination of weight of assumed failure wedge. (a) Elevation, (b) Plan section of wedge

3.3.3 Computation of forces acting on the anchor block

Equation (3.8) or (3.10) can be used to determine the pullout capacity of anchor block in chohesionless soil. As mentioned earlier, total weight W in Eq. (3.8) consists of four weight components of block and wedge. These weight components along with other contributing forces in Eq. (3.8) can be determined as follows:

Weight of wedge, W_w:

Referring to Figure 3.4, a small elemental strip of thickness dz at a height of z from the base of the block is considered. At this depth level the width and the length of the

elemental strip can be expressed as $z\tan\beta$ and $L + 2\,z\tan\alpha\,\tan\beta$ respectively. Thus, the elemental weight, dW_w of the wedge can be obtained as follow

$$dW_w = \;'(L + z\tan\alpha\,\tan\beta)\,(z\tan\beta)dz \tag{3.11}$$

Integrating of Eq. (3.11) over $z = 0$ to $z = B$ gives

$$W_w = \int_0^B \;'(L + z\tan\alpha\,\tan\beta)(z\tan\beta)dz \tag{3.12}$$

$$= \;'\left[\frac{LB^2\tan\beta}{2} + \frac{B^3\tan^2\beta\,\tan\alpha}{3}\right] \tag{3.13}$$

$$= \;'B^2\left[\frac{L\tan\beta}{2} + \frac{B\tan^2\beta\,\tan\alpha}{3}\right] \tag{3.14}$$

Weight of the surcharge above wedge, W_q:

$$W_q = \;'(H - B)\left[\frac{L + L + 2B\tan\alpha\,\tan\beta}{2}\right]B\tan\beta \tag{3.15}$$

$$\text{Or, } W_q = \;'B(H - B)(L + B\tan\alpha\,\tan\beta)\tan\beta \tag{3.16}$$

Weight of the block anchor, W_b:

$$W_b = \;'_b BLt \tag{3.17}$$

Weight of soil above the block anchor, W_S:

$$W_s = \;'(H - B)Lt \tag{3.18}$$

Normal force at the side of the wedge, F_{sn}:

$$F_{sn} = \frac{K_0\;'B^2\left(H - \frac{2B}{3}\right)\tan\beta}{2\cos\alpha} \tag{3.19}$$

Friction force at the side of the wedge, F_{sf}:

$$F_{sf} = F_{sn}\tan\varphi' \tag{3.20}$$

Resultant active thrust, P_a:

$$P_a = K_a\;'LB\left(H - \frac{B}{2}\right) \tag{3.21}$$

Friction force at the top of the block, F_t:

$$F_t = W_s\tan\,_t \tag{3.22}$$

Friction force at the bottom of the block, F_b:

$$F_b = N\tan\,_b \tag{3.23}$$

Friction force at two sides of the block, F_s:

$$F_s = 2K_0\;'\left(H - \frac{B}{2}\right)\tan\,_s Bt \tag{3.24}$$

Where,

φ' = effective angle of internal friction of soil

$'$ = effective unit of soil

$'_b$ = effective unit weight of concrete block = 23.6 kN/m³

α = angle of side flanks of the wedge = $\varphi'/2$ (Reese, et al., 1974)

β = angle of Rankine passive failure surface with the vertical face of anchor block = $45^o + \varphi'/2$

K_a = coefficient of active lateral earth pressure $= (1 - sin\varphi')/(1 + sin\varphi')$

K_o = coefficient of lateral earth pressure at rest $= 1 - sin\varphi'$ (Jaky, 1948)

δ_t = angle of friction between soil and top surface of the block

δ_b = angle of friction between soil and bottom surface of the block

δ_s = angle of friction between soil and side surface of the block

The value or formulae indicated with the above parameters are used while calculating the pullout capacity of anchor block using Eq. (3.8) or Eq. (3.10). It was reported that the anchor block accelerates in the vertically upward direction on the verge of failure (Naser, 2006; Kame, et al., 2012). Consequently, friction force at the bottom of the block (F_b) is assumed to be zero (as $N = 0$). On the other hand, $\delta_t = \delta_s = 20^o$ is preferred to determine F_t and F_s respectively (Bowles, 1997).

3.4   Comparison with the Experimental Results

The anchor and soil parameters of experimental studies conducted by Duncan and Mokwa (2001), Naser (2006) and Mostofa (2013) are presented in Table 3.1. The experimental results of these studies as shown in the second column of Table 3.2 have been used to validate the proposed equations. In addition, pullout capacity were calculated using other theoretical approaches, e.g. Ovesen and Stromann (1972), NAVFAC DM 7.02 (1986), BS 8006 (1995), Ghaly (1997), Bowles (1997) and Naser (2006) and the percentage errors of these methods with respect to experimental results are also shown in the same table. Rankine's lateral earth pressure theory was preferred when required during

calculation process. For a better understanding of the relative predictive accuracy of the proposed method, a cumulative frequency distribution of data corresponding to the percentage error is presented in Table 3.3. Absolute values of the percentage errors were used during frequency distribution, and their average values for each method, which is statistically defined as Mean Absolute Percentage Error (MAPE), were calculated and shown in Table 3.4 in ascending order.

Table 3.1 Anchor block and soil parameters

Author	H (mm)	t (mm)	B (mm)	L (mm)	φ (deg.)	γ (kN/m³)	Soil type	Exp. type
Duncan and Mokwa (2001)	1100	900	1100	1900	50.0	21.20	Gravel	Field
Naser (2006)	300	150	150	150	43.5	17.40	Sand	Lab.
	300	150	150	150	43.5	19.60	Sand	Lab.
	300	150	150	150	43.5	10.90[1]	Sand	Lab.
Mostofa (2013)	475	75	150	150	37.2	14.74	Sand	Lab.
	475	75	150	150	43.9	15.62	Sand	Lab.
	475	75	150	150	44.8	17.51	Sand	Lab.

[1]Submerged unit weight of soil calculated as= (20.7-9.8) kN/m³= 10.90 kN/m³.

Although rigorous conclusion may not be drawn from limited number of test data (e.g. 7 test results used in this case), this comparison imparts some useful information regarding the suitability of different methods at different conditions. For example, when compared to experimental value reported by Duncan and Mokwa (2001), the methods proposed by NAVFAC DM 7.02 (1986), BS 8006 (1995), Ghaly (1997) give errors more than 50% (Table 3.2). Duncan and Mokwa (2001) measured anchor block bearing against compacted gravel backfill near ground surface.

Naser (2006) performed one laboratory test on 100% saturated sandy soil to observe the effect of degree of saturation on pullout resistance of anchor. The error with respect to this test result for methods proposed by Ovesen and Stromann (1972), NAVFAC DM 7.02 (1986) and BS 8006 (1995) is also more than 50%. The remaining 5 test results were conducted on poorly graded unsaturated sand. Each of the method discussed here, except proposed method, gives error more than 50% at least twice (Table 3.3).

Table 3.2 Comparison of theoretical predictions of pullout capacity with experimental results for vertical anchor block

Authors	Exp. results	Proposed Method Eq. (3.8)		Proposed Method Eq. (3.10)		Ovesen and Stromann (1972)		NAVFAC DM 7.02 (1986)		BS 8006 (1995)		Ghaly (1997)		Bowles (1997)		Naser (2006)	
	P_u (kN)	P_u (kN)	% error	P_u (kN)	% error	P_u (kN)	% error	P_u (kN)	% error	P_u (kN)	% error	P_u (kN)	% error	P_u (kN)	% error	P_u (kN)	% error
Duncan and Mokwa (2001)	410.0	412.0	0.5	396.0	-3.4	427.0	4.1	768.0	87.3	735.0	79.2	190.0	-53.6	233.0	-43.2	297.0	-27.6
Naser (2006)	1.3	1.3	0.0	1.2	-7.7	1.9	46.1	1.8	38.5	1.9	46.2	1.0	-23.1	0.6	-53.8	1.3	0.0
	2.3	1.5	-34.8	1.4	-39.1	2.0	-13.0	2.0	-13.0	2.2	-4.3	1.1	-52.2	0.7	-69.6	1.5	-34.8
	0.7[1]	0.8	14.3	0.7	0.0	1.5	114.3	1.1	57.1	1.2	71.4	0.6	-14.3	0.4	-42.9	0.8	14.3
Mostofa (2013)	1.9	1.2	-36.8	1.1	-42.1	2.2	15.8	1.5	-21.1	2.2	15.8	2.1	10.5	0.6	-68.4	1.8	-5.3
	2.1	1.9	-9.5	1.7	-10.5	3.1	47.6	3.0	42.9	3.1	47.6	1.8	-14.3	0.9	-57.1	3.6	71.4
	2.3	2.2	-4.3	2.0	-13.0	3.5	52.2	3.8	65.2	3.6	56.5	1.9	-17.4	1.0	-56.5	4.4	91.3

[1]Pullout resistance at 100% saturated condition

Table 3.3 Cumulative frequency distribution of errors for vertical anchor block

Absolute % error	Proposed Method Eq. (3.8)		Proposed Method Eq. (3.10)		Ovesen and Stromann (1972)		NAVFAC DM 7.02 (1986)		BS 8006 (1995)		Ghaly (1997)		Bowles (1997)		Naser (2006)	
	Frequency	Cum. Frequency	Frequency	Cum. Frequency	Frequency	Cum. Frequency	Frequency	Cum. Frequency	Frequency	Cum. Frequency	Frequency	Cum. Frequency	Frequency	Cum. Frequency	Frequency	Cum. Frequency
0-10	4	4	3	3	1	1	0	0	1	1	0	0	0	0	2	2
10-20	1	5	2	5	2	3	1	1	1	2	4	4	0	0	1	3
20-30	0	5	0	5	0	3	1	2	0	2	1	5	0	0	1	4
30-40	2	7	1	6	0	3	1	3	0	2	0	5	0	0	1	5
40-50	0	7	1	7	2	5	1	4	2	4	0	5	2	2	0	5
>50	0	7	0	7	2	7	3	7	3	7	2	7	5	7	2	7

Table 3.4 Mean absolute percentage error (MAPE) of different methods

Sl. No.	Authors	MAPE
1	Proposed Method Eq. (3.8)	14.3
2	Proposed Method Eq. (3.10)	16.5
3	Ghaly (1997)	26.5
4	Naser (2006)	35.0
5	Ovesen and Stromann (1972)	41.9
6	BS 8006 (1995)	45.9
7	NAVFAC (1986)	46.4
8	Bowles (1997)	55.9

Ovesen and Stromann (1972) overestimated the test results in most of cases. They considered friction between wall and soil during upward movement of passive wedge, which in turn contributes favourably in pullout capacity. However, anchor block moves together with the passive wedge resulting no shear displacement between wall and passive wedge (Duncan and Mokwa, 2001). Thus, the test results are smaller than their predictions for anchor block. BS 8006 (1995) also overestimated test results in 6 out of 7 cases significantly. BS 8006 (1995) assumes that pullout resistance of anchor is 4 times the passive resistance of soil, while experimental studies by Mostofa (2013) indicated that this coefficient is always less than 4.

In other circumstances, Bowles (1997) method underestimated the each test results significantly. He used conventional earth pressure theories assuming implicitly that the conditions at all cross sections along the length of a structure are the same, ignoring the influence of the different conditions at the ends of the structure which contributes greatly on pullout resistance of anchor.

Ghaly's (1997) empirical equation underestimated test results twice by more than 50% (Table 3.2) for relatively denser soil (Table 3.1). He used the results of 104 laboratory tests, 15 centrifugal tests, and 9 field tests to propose this empirical correlation, where unit weight and internal friction angle of soil ranged from 14 to16 kN/m^3 and 34° to 38.5^o respectively. It is expected that more deviation from the range of test parameters used to derive the empirical correlation causes more errors. This is probably the reason for highest error corresponding to the test results of Duncan and Mokwa (2001), where unit weight and internal friction angle of soil were 21.2 kN/m^3 and 50° respectively.

The proposed method, Eq. (3.8) or Eq. (3.10) gives absolute error in the range, 0 to 15% in 5 out of 7 cases. For remaining cases, it underestimates the actual results by 30% to 45%. It indicates the better predictive capability of the proposed method as compared to the other methods for varied parameters of soil and anchor. The mean absolute percentage error (MAPE), as shown in Table 3.4, is lowest as compared to the other methods discussed here.

The prediction of pullout capacity by Eq. (3.10) is slightly smaller than Eq. (3.8). Thus, the frictional resistance offered by thickness of the anchor block and side wedge is insignificant compared to the passive resistance that derived from the weight of passive wedge. Although the accuracy level of both proposed equation does not differ much, Eq. (3.10) is preferable for its simplicity and offers quick estimation of pullout capacity of anchor block using charts which will be presented in the later section of this chapter.

3.5 Break-Out Factors

It is always convenient to use graphical representation of a mathematical model that consists of many variables or parameters. An effort has been made here to develop charts; those may be used to calculate the pullout capacity of anchor block instead of using Eq. (3.10) directly. For this purpose, a dimensionless parameter called break-out factor, N is introduced that may be defined as the ratio of P_u and $'B^3$.

$$N = \frac{P_u}{'B^3} = \frac{W/tan\,(\beta - \varphi')}{B^3} \tag{3.25}$$

Let us consider a cube shaped anchor block (i.e. $B = L = t$), for which the weight components of block and wedge can be expressed as:

$$W_w = \ 'B^3 \left[\frac{tan\beta}{2} + \frac{tan^2\beta\,tan\alpha}{3}\right] \tag{3.26}$$

$$W_q = \ 'B^3 \left(\frac{H}{B} - 1\right)(1 + tan\alpha\,tan\beta)tan\beta \tag{3.27}$$

$$W_b = 1.5\ 'B^3 \tag{3.28}$$

$$W_s = \ 'B^3 \left(\frac{H}{B} - 1\right) \tag{3.29}$$

Summing up Eq. (3.26), Eq. (3.27), Eq. (3.28) and Eq. (3.29) to obtain W

$$W = \ 'B^3 \left[\frac{tan\beta}{2} + \frac{tan^2\beta\,tan\alpha}{3} + \left(\frac{H}{B} - 1\right)(1 + tan\alpha\,tan\beta)tan\beta\right.$$
$$\left. + 1.5 + \left(\frac{H}{B} - 1\right)\right] \tag{3.30}$$

Now, substituting the value of W from Eq. (3.30) into Eq. (3.25) for N:

$$N = \frac{1}{\tan(\beta - \varphi')}\left[\frac{\tan\beta}{2} + \frac{\tan^2\beta\,\tan\alpha}{3}\right.$$

$$\left.+ \left(\frac{H}{B} - 1\right)(1 + \tan\alpha\,\tan\beta)\tan\beta + 1.5 + \left(\frac{H}{B} - 1\right)\right] \quad (3.31)$$

Similarly, for $B = L = 2t$, the break-out factor N will be:

$$N = \frac{1}{\tan(\beta - \varphi')}\left[\frac{\tan\beta}{2} + \frac{\tan^2\beta\tan\alpha}{3}\right.$$

$$\left.+ \left(\frac{H}{B} - 1\right)(1 + \tan\alpha\,\tan\beta)\tan\beta + .75 + .5\left(\frac{H}{B} - 1\right)\right] \quad (3.32)$$

From Eq. (3.31) and Eq. (3.32), it is observed that N is the function of H/B and φ' only, and the graphical representation of these equations yield a series of straight lines as depicted in Figure 3.5 and Figure 3.6 respectively. It is worth to mention that unit weight of concrete was assumed as 1.5 times unit weight of soil in Eq. (3.28). However, such assumption causes insignificant amount of error. For example, $N= 63.45$ (for $H/B=5$, $'=45°$, $B = L = t$ and $\gamma_{block}=23.6$ kN/m^3) when $\gamma_{block} = \gamma_{soil}$; while for similar condition $N=65.86$ for $\gamma_{block} = 2\gamma_{soil}$. Thus, the later value is greater by only 3.8% than the previous value.

It is to be noted that while using Figure 3.5 and Figure 3.6, liner interpolation may be performed for intermediate values of φ'. Also, submerged unit of soil should be used when the degree of saturation is 100% or, water table is located at ground surface.

Example 1 $H= 5$ m, $B=L=t=1$ m, $\varphi'=45°$, $'=18$ kN/m^3

     From Figure 3.5, $N=65$ for $H/B=5$ and $\varphi'=45°$

     Hence, $P_u=N\,'B^3=(65)(18)(1^3)=1170$ kN

Example 2 $H= 5$ m, $B=L=2t=1$ m, $'=43°$, $'=18$ kN/m^3, Water table at ground surface.

     Interpolating for $\varphi'= 43°$ and $H/B=5$, Figure 3.6 yields $N= 51$

     $\gamma_{sub}=\gamma\,'= (18-9.8)$ kN/m^3=8.2 kN/m^3

     Hence, $P_u=N\,'B^3=(51)(8.2)(1^3)=418$ kN
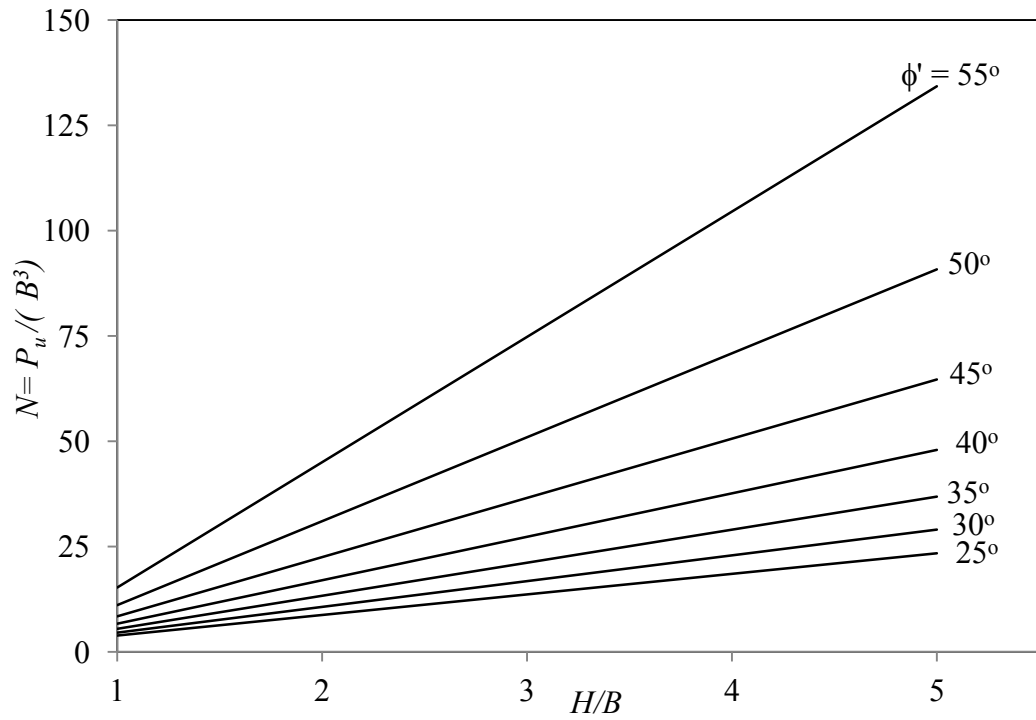
Figure 3.5 Break-out factors for anchor block in cohesionless soil (for $B = L = t$)
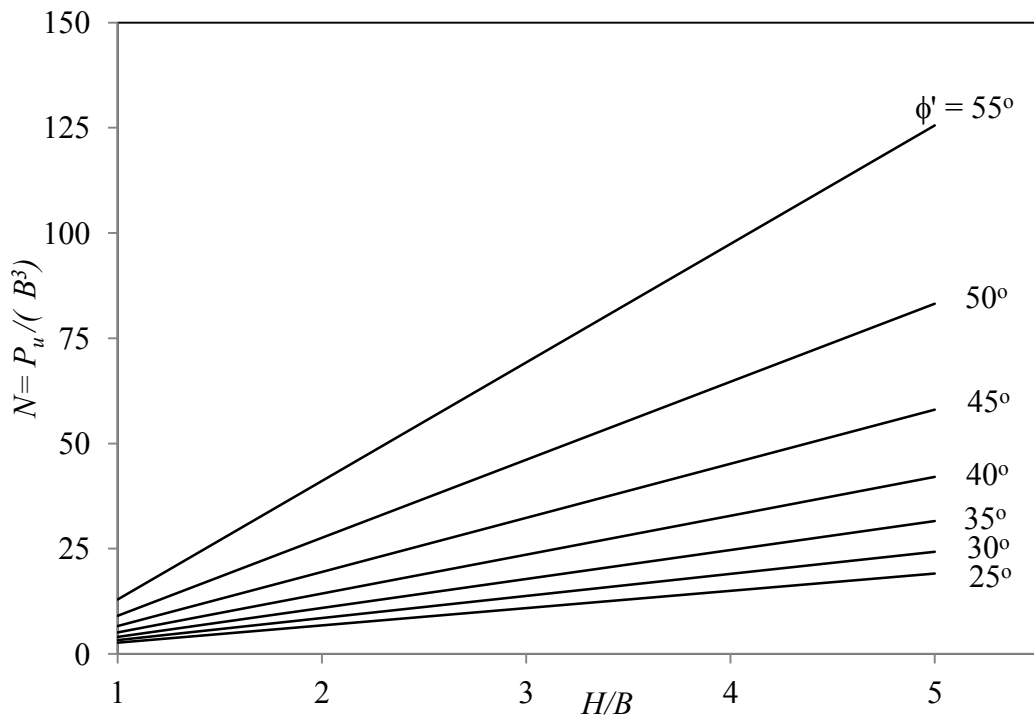
Figure 3.6 Break-out factors for anchor block in cohesionless soil (for $B = L = 2t$)

3.6   Concluding Remarks

Proposed analytical method was first formulated considering all possible contributing forces in the anchor block and wedge. Subsequently, it was simplified neglecting the comparatively less influencing parameters intended for ease. Furthermore, simplified method was facilitated with charts for quick estimation of the pullout resistance of anchor block for most frequently used shapes, cube shaped and square shaped with half of height/length of block as thickness. In most of the cases, the predictions of this method show a very close agreement with experimental results. The prediction appears to be better than other methods for varied condition of soil. The effect of ground water table can also be taken into consideration while calculating the pullout resistance. Although the proposed analysis uses equilibrium of passive wedge and ignores the shearing above the anchor block, it is improved with a proper selection of angle φ' and α. Since limited field and laboratory observations were available in the literature for fair comparison of the different methods, sufficient field observations are required to develop confidence among the users about the suitability of the proposed method along with other methods discussed here.

CHAPTER 4
NUMERICAL ANALYSIS OF ANCHOR BLOCK

4.1   General

In the previous Chapter, proposed theoretical method was verified with limited number of experimental studies. Since the cost of performing experimental tests on each and every field problem combination is excessive, it is necessary to perform numerical analysis for economy, time and safety. Moreover, the results obtained from experimental testing alone are generally problem specific. This is particularly the case in geomechanics where we are dealing with a highly nonlinear material which often displays pronounced scale effects. As a result, it is often difficult to extend the findings from experimental data to full scale problems with different material or geometric parameters. Therefore, an effort has been made here to study the pullout resistance of anchor block numerically, which substantiates the theoretical method proposed in the last chapter. This chapter mainly focuses on study of the effects of aspect ratio, ground water table and embedment depth ratio on pullout resistance of anchor block. However, it is essential to approximate the behaviour of soil as realistic as possible. If the input parameters are sufficiently precise, then the output results of the numerical analysis are usable.

Figure 4.1 Problem definition (a) Front view, (b) Side view of an anchor

4.2   Problem Definition

An anchor block of length L, height B and thickness t installed in sand with an embedment depth of H as schematized in Figure 4.1 was simulated in this study. During the

installation, the soil in the vicinity of the anchor block can be disturbed. However, the effects of disturbance on capacity were not considered in this study; instead, the simulations were performed for a wished-in-place anchor block. The anchor block was loaded at the centre of passive side as shown in Figure 4.1 (b). The effects of aspect ratio (L/B) was observed using five different sizes of anchor block, and the ground water level is located eight different levels for a given anchor block to study the impact of ground water table on pullout capacity. Additionally, the anchor block is placed at nine different depths to investigate the variation of pullout capacity of anchor block with embedment ratio (H/B). The properties of anchor block and soil are presented in the following sections.

4.3   Finite Element Model

The 3D Finite Element (FE) program, PLAXIS 3D Foundation (Version 1.1), was used to represent the soil-structure system. The system is symmetrical with respect to the z-axis. The soil is assumed isotropic and homogenous with Mohr-Coulomb yield criterion and is defined by the cohesion value C, angle of internal friction φ, and dilatancy angle ψ.
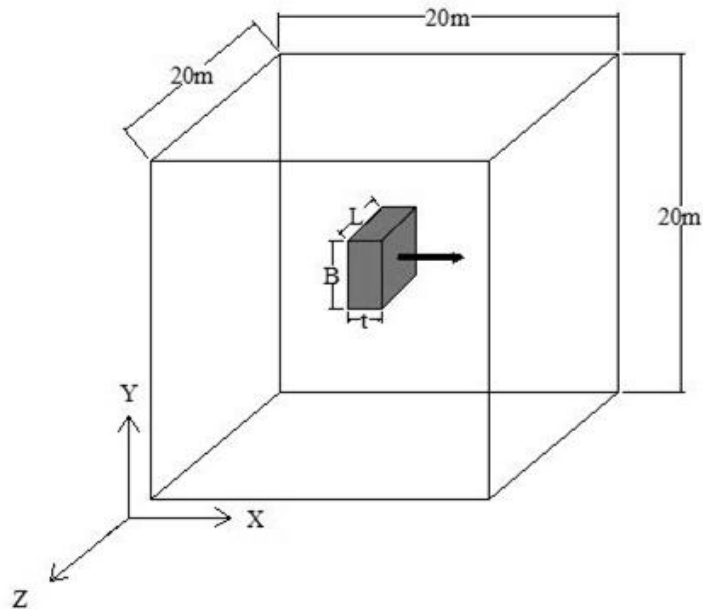
Figure 4.2 Geometry of Finite Element model

The selected dimensions of the model were large enough to prevent any restriction of propagation of stresses and strains. Although analyses would take more time, the stress and strain distribution in the soil because of different pullout loads in different positions can be observed precisely. Considering the stress and strain propagation, dimensions of the model

40

to avoid any restrictions at the boundaries were computed through trial and error. Hence, a homogeneous and isotropic soil domain with a width of 20 m, height of 20 m, and depth of 20 m was modelled (Figure 4.2).
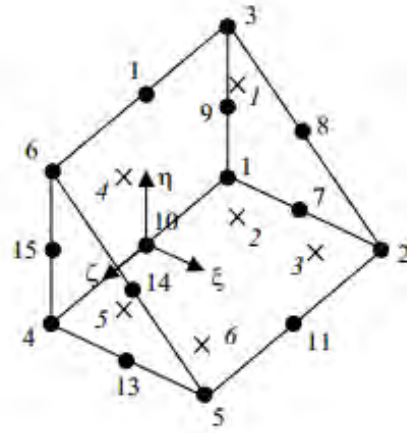
Figure 4.3 Distribution of nodes and stress points in a 15-node wedge element

The wedge elements used in the 3D Foundation program consists of 15 nodes. The distribution of nodes over the elements is shown in Figure 4.3. Adjacent elements are connected through their common nodes. During a finite element calculation, displacements (u_x, u_y and u_z) are calculated at the nodes. Nodes may be pre-selected for the generation of load-displacement curves.
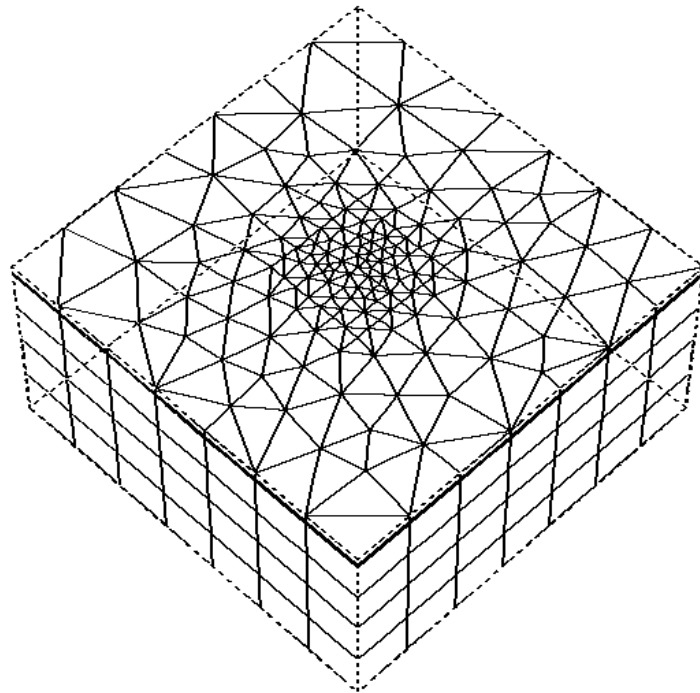
Figure 4.4 Distribution of elements around the anchor block

41

As mentioned earlier, all of the boundaries were considered far enough to prevent stress reflection. In fact, the dimensions of the model have been selected in a way that the stress and displacement gradients would decrease and become zero by getting close to the boundaries. To obtain more accurate results, elements were kept very small near the anchor block, increasing gradually in size and moving away from the block (Figure 4.4).

PLAXIS automatically imposes a set of general fixities to the boundaries of the geometry model. These conditions are generated according to the following rules:

(i) Vertical model boundaries with their normal in x-direction (i.e. parallel to the y plane) are fixed in x-direction ($u_x = 0$) and free in y- and z-direction, as shown in Figure 4.2.

(ii) Vertical model boundaries with their normal in z-direction (i.e. parallel to the x-y-plane) are fixed in z-direction ($u_z = 0$) and free in x- and y-direction.

(iii) Vertical model boundaries with their normal neither in x- nor in z-direction (skew boundary lines in a work plane) are fixed in x- and z-direction ($u_x = u_z = 0$) and free in y-direction.

(iv) The model bottom boundary is fixed in all directions ($u_x = u_y = u_z = 0$).

(v) The 'ground surface' of the model is free in all directions.

Load-displacement curves can be used to visualise the relationship between the applied loading and the resulting displacement of a certain point in the geometry. In PLAXIS output-program, the x-axis relates to the displacement of a particular node, and the y-axis contains data relating to load level. The latter is related with the value of ΣM_{stage} in the following way: Applied load = Total load applied in previous phase + ΣM_{stage} times (Total load applied in current phase minus Total load applied in previous phase). At the start of a staged construction calculation, the multiplier that controls the staged construction process, ΣMstage, is zero and this multiplier is stepwise increased to 1.0. When ΣM_{stage} has reached the value of 1.0, the current phase is finished. However, if a staged construction calculation is not properly finished, i.e. the multiplier ΣM_{stage} is less than 1.0 at the end of a staged construction analysis. To obtain the load-displacemnt curve, first the ΣM_{stage} - displacement curve was generated in the output program. Then, the data from the curve was copied to a spreadsheet program. The Applied load was calculated simply multiplying the ΣM_{stage} with

the input-load in the loading phase, as the Total load applied in previous phase was zero in this case. A sample calculation is provided in the APPENDIX, where the applied load and the corresponding displacement was determined from Finite Element analysis of the experimental study conducted by Naser (2006).

4.3.1 Modelling of anchor block

An anchor block of 0.4 m length, 0.4 m height and 0.4 m thickness was modelled first. Analyses were also performed for different lengths to observe the effect of aspect ratio on pullout capacity. By modelling the block as elastic-perfectly plastic material and also as rigid body, it was found that the pullout capacity does not vary significantly with these modelling techniques. However, the FE model with the block as a rigid body is computationally very efficient. Therefore, the block was considered as a rigid body in the FE analyses. The geometry and the properties of the anchor block used in the study are presented in the Table 4.1. This geometry along with the soil parameters shown in Table 4.1 is referred as "base case" in the following sections.

Table 4.1 Geometry and mechanical properties in FE modelling

Anchor Block	Length (L)	0.4 m
	Height (B)	0.4 m
	Thickness (t)	0.4 m
	Modulus of elasticity (E_b)	2×10^7 kN/m^2
	Poisson's ratio ($_b$)	0.2
	Unit weight of anchor block(γ_b)	23.6 kN/m^3
Cohesionless Soil	Angle of internal friction (φ')	35°
	Angle of dilation (ψ)	5°
	Young's modulus (E_s)	60,000 kN/m^2
	Poisson's ratio ($_s$)	0.3
	Cohesion (c')[1]	0.5 kN/m^2
	Unit weight of soil (γ_s)	15.73 kN/m^3
	Interface reduction factor (R_{inter})	0.5

[1]Small cohesion is required to be defined in PLAXIS FE analysis. For sand, in this study a very small value of c'= 0.5 kN/m^2 was used.

4.3.2 Modelling of cohesionless soil

The cohesionless soil was modelled using the built-in Mohr-Coulomb model available in the PLAXIS FE software. While loading, cohesionless soil was treated as drained homogeneous material. The unit weight and the angle of internal friction of soil were assumed as 15.73 kN/m^3 and 35° respectively for most of the cases. The properties of the soil used in the FE analysis are shown in Table 4.1.

4.3.3 Interface behaviour

In PLAXIS, the soil/anchor interaction is modelled by choosing a suitable value for the strength reduction factor (R_{inter}) in the interface, which is defined as $R_{inter} = tan\varphi_i / tan\varphi$. Where, φ_i and φ are the friction angle for interface and soil respectively. This factor relates the interface strength (anchor friction) to the soil strength (friction angle and cohesion). The value R_{inter} varies between 0 and 1 depending upon surface roughness, mean particle size of sand and method of installation (CFEM, 2006; Tiwari, et al., 2010). In general, for real soil-structure interaction the interface is weaker and more flexible than the associated soil layer, which means that the value of R_{inter} should be less than 1. Suitable values for R_{inter} for the case of the interaction between various types of soil and structures in the soil can be found in the literature. In this study, friction angle for interface (φ_i) was assumed as 20° (Das, 1995; Bowles, 1997). Thus, the approximate value of interface reduction factor (R_{inter}) was calculated as 0.5 for =35°.

4.3.4 Modulus of elasticity of sand

The Young's modulus of sand, E_s, can be expressed as a function of mean effective stress, p', as, $E_s = Kp_{atm} (p'/p_{atm})^n$ (Janbu, 1963; Hardin and Black, 1966); where, K and n are two material parameters, p_{atm} is the atmospheric pressure = (100 kPa). The displacement of an anchor block due to pullout force may be obtained from FE model. This displacement depends considerably on the value of modulus of elasticity of soil, E_s. Since the study of such displacement is out of scope of the present research work, no attempt has been taken to vary E_s with p', rather a constant value of E_s = 60 MPa was used.

4.3.5 Dilatancy angle of cohesionless soil

The angle of dilation (ψ) controls an amount of plastic volumetric strain developed during plastic shearing and is assumed constant during plastic yielding. The value of $\psi = 0$ corresponds to the volume preserving deformation while in shear. For sands, the angle of dilation depends on the angle of internal friction. In this study, the value of dilation angle was estimated using PLAXIS 3D reference manual (version 1) which recommends to determine the value of dilation angle as $\psi = \phi - 30^{o}$ for non-cohesive soils (sand, gravel) with the angle of internal friction, $\varphi > 30^{o}$.
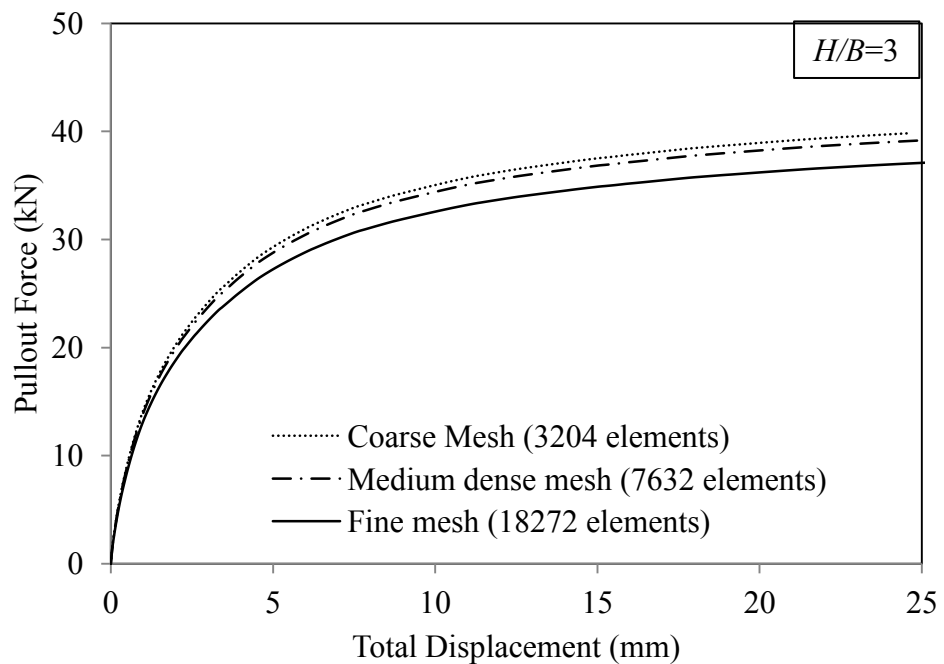
Figure 4.5 Mesh sensitivity analysis

4.4   Results and Discussions

4.4.1 Mesh sensitivity analysis

In general, smaller FE mesh yields more accurate results but computationally expensive. For efficient modelling, small elements are used near the block. The size of the elements is increased with increase in distance from the block as shown in Figure 4.4. Similarly, the element size is increased with distance from the bottom of the block. To select the optimum mesh, several trial analyses are conducted with different mesh sizes. The force-displacement curves for three different sizes of mesh are shown Figure 4.5 for the base case

(Table 4.1) with the embedment depth ratio, $H/B=3$. As shown in Figure 4.5, the calculated pullout force is smaller with fine mesh than that of with coarse mesh. In this study, the fine mesh was selected to perform the analyses as it is more accurate, although it is recognized that it is computationally expensive.

Table 4.2 Anchor block and soil parameters to investigate the effect of aspect ratio

H (m)	t (m)	B (m)	L (m)	φ (deg.)	γ (kN/m^3)	P_u (kN)	L/B	N $=P_u/(\ BLt)$
1.2	0.4	0.4	0.4	35	15.73	28	1	27.8
1.2	0.4	0.4	0.8	35	15.73	50	2	24.8
1.2	0.4	0.4	1.2	35	15.73	70	3	23.2
1.2	0.4	0.4	2.0	35	15.73	112	5	22.3
1.2	0.4	0.4	3.6	35	15.73	200	9	22.1

4.4.2 Effect of aspect ratio

While the soil properties influence the pullout capacity significantly, the size and shape of the anchor has also considerable influence on ultimate pullout resistance of an anchor block (Das, 1990; Rowe and Davis, 1982). The length (L) of the anchor block is gradually increased from the base case to observe the effect of anchor shape on ultimate capacity. However, the other geometries of the anchor block and soil parameters remain same as base case, which is presented in Table 4.2.
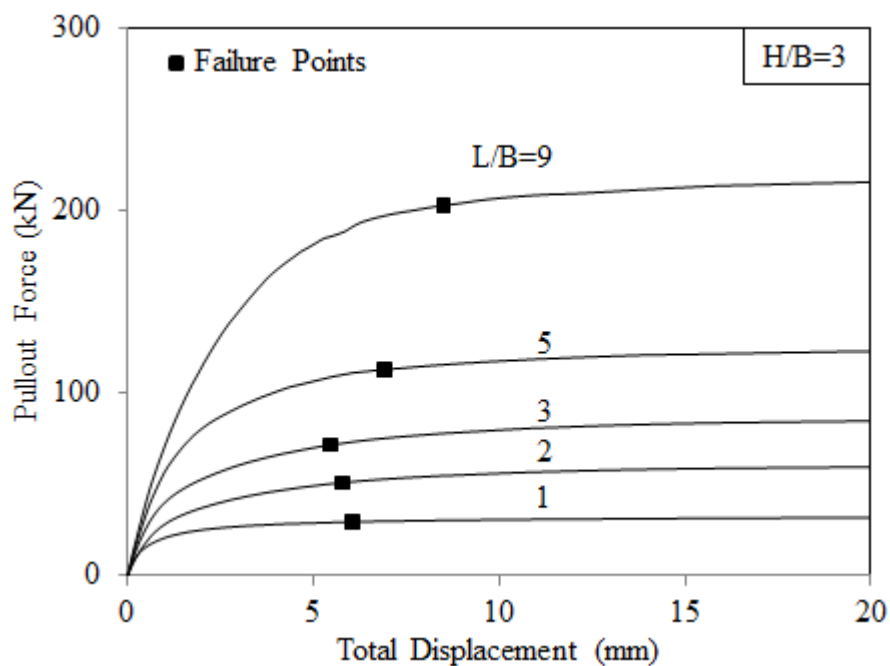
Figure 4.6 Load-displacement curve for the study of the effect of aspect ratio (L/B)

46

The variation of pullout force with total displacement for embedment depth ratio $H/B =3$, along the direction of pulling is shown Figure 4.6. In this study, the load displacement curves do not show any peak; rather the pullout force is increasing very gradually after plastic yielding. Therefore, ultimate capacity is defined by adopting failure points, as shown in Figure 4.6, after which the load-displacement diagrams become practically linear (Neely, et al., 1973; Das, 1990). This method was also utilized by Dickin and King (1997) and Ghaly (1997) and they found more consistent results with experimental studies than other alternative methods.

The impact of aspect ratio (L/B) on ultimate capacity for an anchor block with $H/B = 3$, is presented in Figure 4.7. Here, the pullout capacity is expressed as a dimensionless parameter called break-out factors (N) similar to the last chapter, which is defined as the ratio of P_u and γBLt. Figure 4.7 indicates that decreasing aspect ratio results increasing break-out factor (relative to $L/B =9$) of 26%, 12%, 5% and 1% for L/B ratios of 1, 2, 3 and 5 respectively. Hence, the effect of shape is considerable for $L/B \leq 2$ and is of insignificant importance for $L/B \geq 5$. This is attributed to fact that the boundary conditions at the ends of a square structure are quite different from those at the center, which contributes greatly on pullout resistance. As the aspect ratio increases, the influence of boundary conditions decreases, and plain strain results (2D analysis) will be more applicable for large aspect ratios. Figure 4.7 also indicates that a rectangular anchor block with $L/B \geq 5$ should be treated as strip anchor block.
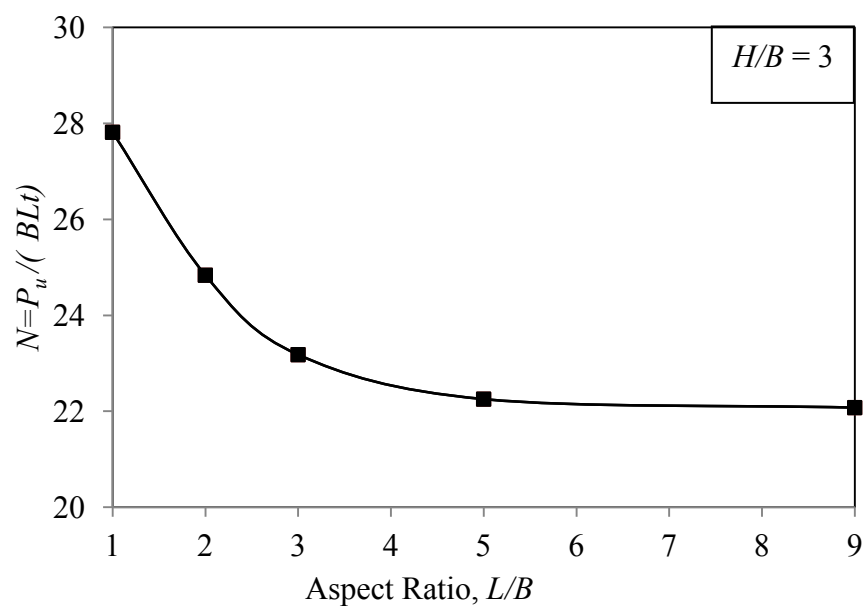
Figure 4.7 Effect of aspect ratio (L/B) on pullout capacity of anchor

4.4.3 Effect of ground water table

The effect of ground water table can be considered in the analytical method, Eq. (3.8) and Eq. (3.10), derived in the last chapter, when ground water table is located at ground surface. The use of submerged unit weight (γ') instead of bulk unit weight of soil (γ) in the analytical expression is sufficient to account the effect of water table. However, ground water table may be located at any level in the soil layer. Consequently, an effort has been made here to account the influence of ground water table located at any position.

The analysis was performed for the base case, where the anchor block is placed at 1.2 m depth, i.e. H/B=3. The depth of ground water table is denoted by z, as shown in Figure 4.8. All the analyses were conducted for the locations of ground water table at $z/H = 0$, 0.17, 0.33, 0.5, 0.67, 0.83 and 1.00 as presented in Table 4.3. In one circumstances, the water table is kept well below (20 m depth) so that water table has practically no influence on pullout capacity of anchor block, which is referred as dry condition in this section. The pullout capacity for different locations of ground water table is determined from load-displacement curves as depicted in Figure 4.9 and is presented in the Table 4.3.
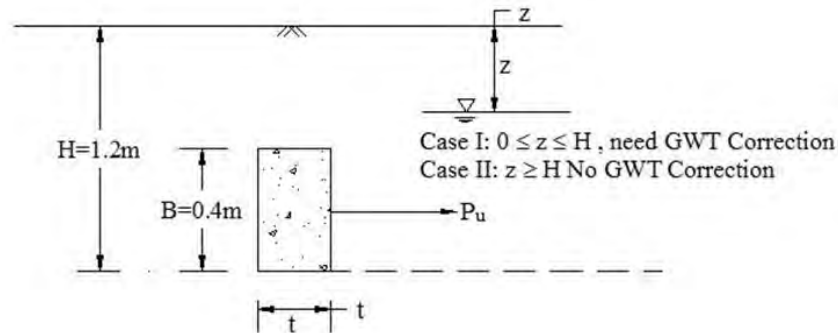
Figure 4.8 Effect of water table and correction factors.

Table 4.3 Correction factors for different locations of ground water table

z (mm)	H (mm)	z/H	$P_{u,GWT}$ (kN)	$P_{u,dry}$ (kN)	$P_{u,GWT}/P_{u,dry}$
0.0	1.2	0.00	14.0	28.0	0.50
0.2	1.2	0.17	18.0	28.0	0.64
0.4	1.2	0.33	22.5	28.0	0.80
0.6	1.2	0.50	25.5	28.0	0.91
0.8	1.2	0.67	27.0	28.0	0.96
1.0	1.2	0.83	27.5	28.0	0.98
1.2	1.2	1.00	28.0	28.0	1.00
Dry cond.	1.2		28.0		
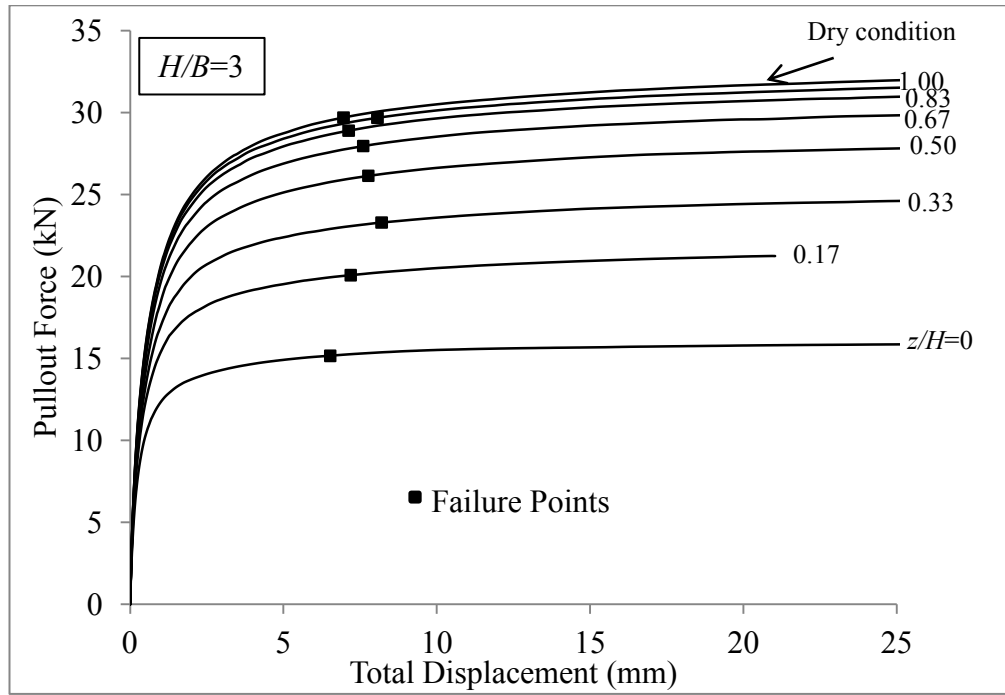
Figure 4.9 Load-displacement curves for different locations of ground water table

The pullout resistance of anchor block, when ground water table is located at the base of the block is same as dry condition in this case (Table 4.3). Thus, the ground water table may not have essentially any influence on pullout resistance of anchor block for the case $z \geq H$. However, the effect of ground water table should be considered, when the water table is anywhere between the ground surface and the base of the anchor block, that is, $0 \leq z \leq H$. The correction factor for water table, defined as the ratio of pullout resistance with ground water table between $0 \leq z \leq H$ to that of dry condition, is determined and presented in Table 4.3. Figure 4.10 shows the variation of correction factor with z/H. In this case, the correction factor was found as 0.5 when water table is at ground surface i.e. $z/H=0$ and the factor is 1 when water table is at the base of anchor block, i.e. $z/H=1$. The variation of correction factor from ground surface to the base of anchor block is not linear, rather concave downward as shown in Figure 4.10. Therefore, an empirical equation is proposed here, which may be used roughly to determine the correction factor for water table. The correction factor should be multiplied with the pullout resistance at dry condition to account the ground water table effect. The considerations on ground water table can be summarized as follow:

Case I: No correction is needed for $z \geq H$.

Case II: Correction should be applied for $0 \leq z \leq H$. Correction factor may be calculated from Eq. (4.1).

$$P_{u,GWT}/P_{u,dry} = -0.6\,(z/H)^2 + 1.1(z/H) + 0.5 \qquad (4.1)$$

Where, $P_{u,GWT}/P_{u,dry}$ is correction factor for water table and (z/H) is the depth ratio at ground water level.
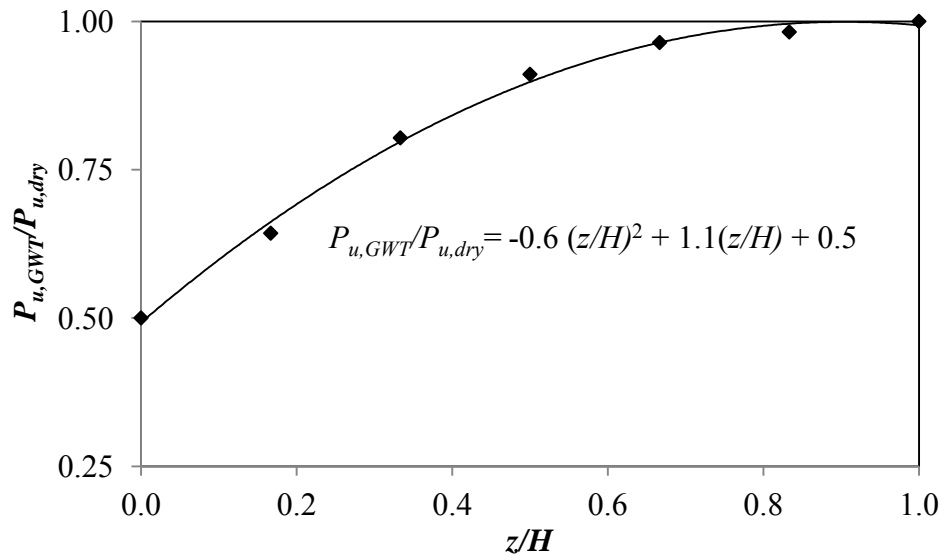
Figure 4.10 Variation of correction factors with the location of ground water table

4.4.4 Effect of embedment depth ratio

In the last chapter, we have seen that the analytical expression, Eq. (3.10) has been facilitated with charts (Figure 3.5 and Figure 3.6) for most frequently used shapes, cube shaped and square shaped with half of height/length of block as thickness. It is observed from Figure 3.5 and Figure 3.6 that the theoretical break out factor, N varies linearly with the embedment depth ratio (H/B) for a given value of angle of internal friction of soil (φ). However, Eq. (3.10) was verified with several test results from literature, which were mostly conducted at shallow depth ($H/B < 4$). The failure mechanism of shallow anchors and deep anchors are not similar. For shallow anchors, the embedment ratio is such that, failure surface reaches the ground surface at limit equilibrium; whereas for deep anchors, the embedment ratio is such that, failure surface does not reach the ground surface at limit equilibrium (Das, 1990). Thus, the suitablity of Eq. (3.10) for greater embedment ratio ($H/B \geq 4$) should be confirmed.

Accordingly, FE analysis with PLAXIS was conducted for the base case, where the anchor block is placed at embedment depth ratio (H/B) of 1 to 9. The pullout capacity for different embedment ratio is determined from load-displacement curves as depicted in Figure 4.11

and is presented in the Table 4.4. The break-out factors (N) were calculated from pullout capacity of anchor block (Table 4.4) and compared with the proposed method, Eq. (3.10) along with other methods suggested by different authors as shown in Figure 4.12.

The FE analyses show that the relationship between the break-out factor and the embedment depth ratio is not linear as depicted in Figure 4.12, instead N increases faster at greater embedment depth ratio. The proposed theoretical method fits better with the FE analysis results than other methods suggested by Naser (2006), Ghaly (1997), BS 8006 (1995) and Ovesen and Stromann (1972) for $H/B \leq 5$. In section 4.6, it will be shown that, the Mohr-coulomb model somewhat overestimates the actual result. Inspite of this fact, the smaller prediction of the proposed method than the FE analyses is significant for greater embedment ratio ($H/B > 5$). For exmple, it predicts nearly half as FE analysis result for $H/B =9$. On the other hand, the methods proposed by BS 8006 (1995) and Naser (2006) show good agreement with the FE anlysis for greater embedment ratio. Thus, it is recommended that the proposed theoretical method, Eq. (3.10) should be used for shallow depth i.e. $H/B \leq 5$.
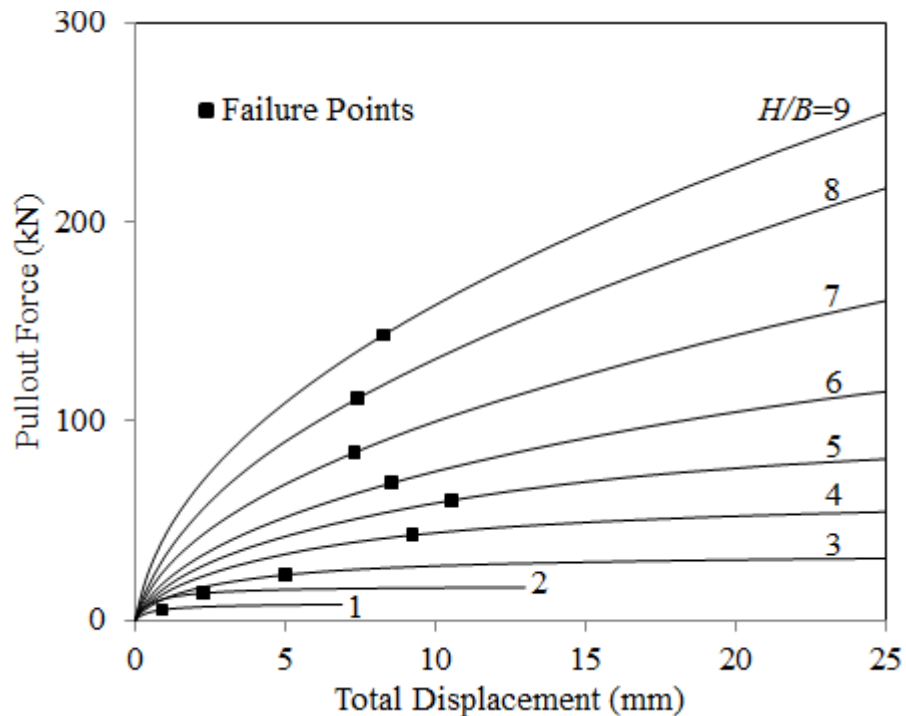
Figure 4.11 Load-displacement curves for different embedment depth ratio

Table 4.4 Pullout resistance of anchor block for different embedment ratio.

H (m)	t (m)	B (m)	L (m)	φ (deg.)	γ (kN/m^3)	P_u kN	H/B	$N = P_u/(\gamma B^3)$
0.4	0.4	0.4	0.4	35	15.73	8	1	7.9
0.8	0.4	0.4	0.4	35	15.73	17	2	16.9
1.2	0.4	0.4	0.4	35	15.73	26	3	25.8
1.6	0.4	0.4	0.4	35	15.73	35	4	34.8
2	0.4	0.4	0.4	35	15.73	50	5	49.7
2.4	0.4	0.4	0.4	35	15.73	65	6	64.6
2.8	0.4	0.4	0.4	35	15.73	85	7	84.4
3.2	0.4	0.4	0.4	35	15.73	110	8	109.3
3.6	0.4	0.4	0.4	35	15.73	140	9	139.1
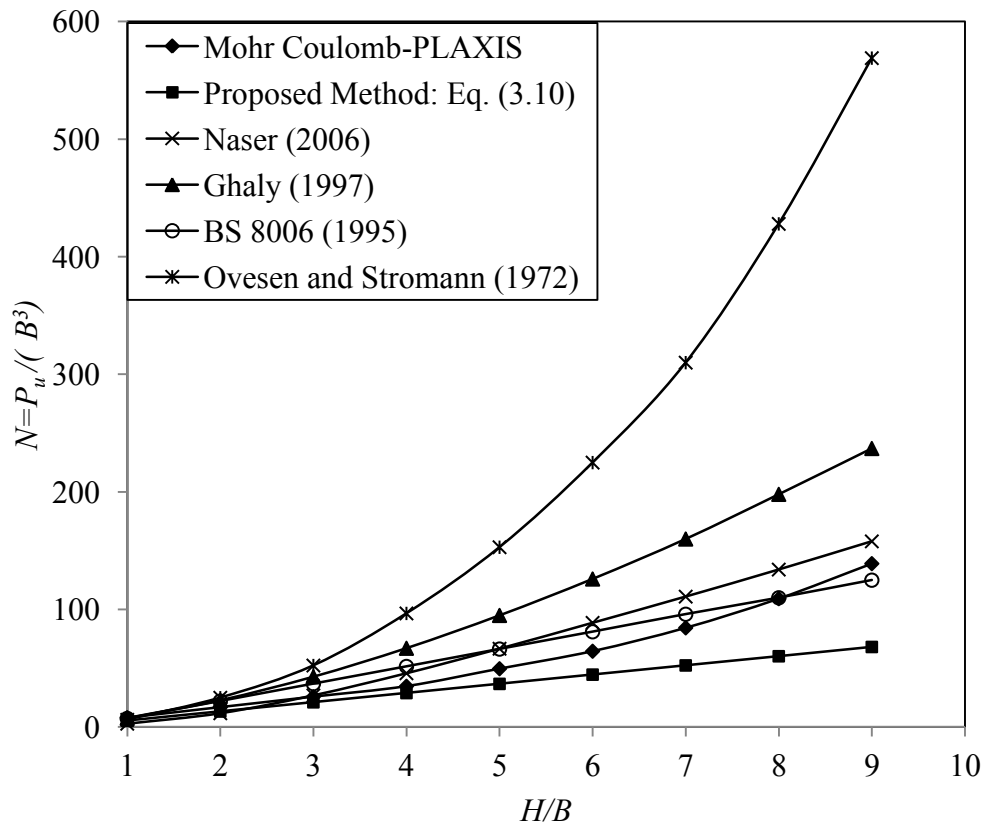
Figure 4.12 Comparison of break-out factors obtained from FE analyses with the proposed method along with other methods suggested by different authors for φ=35°

4.5 Failure Modes of Soil

The complex nature of vertical anchor behaviour, due to the lack of symmetry, has led to a great deal of uncertainty regarding the likely failure patterns at collapse. As a result, it is difficult to predict the capacity of vertical anchors using existing approaches that require

assumptions regarding the shape of the failure surface (Merifield and Sloan, 2006). Such approaches include the limit equilibrium method, the method of characteristics, and any analytical upper bound method.

(a)   (b)
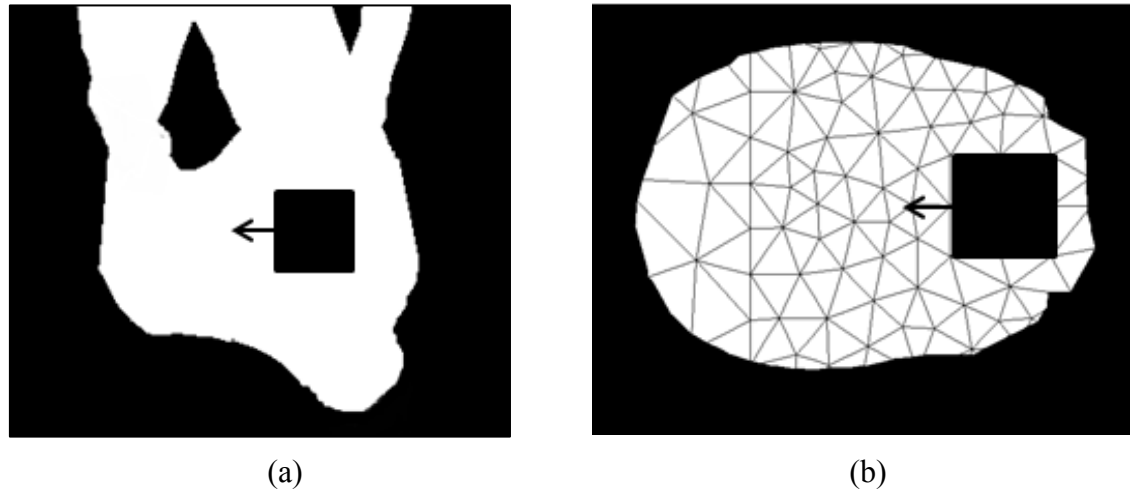
Figure 4.13 Failure modes and zones of plastic yielding for anchor block in cohesionless soils as predicted by PLAXIS for $H/B=3$ and $\varphi=35^{o}$ (a) vertical section and (b) at ground surface
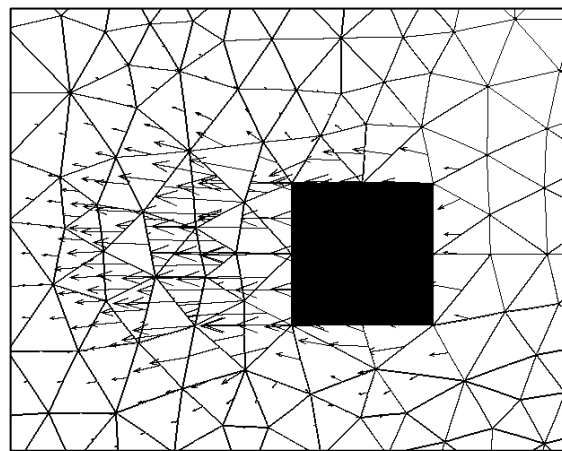
Figure 4.14 Displacement fields during collapse at mid-level of anchor block for $H/B=3$ and $\varphi=35^{o}$

A distinct advantage of the numerical analysis used is that the form of the failure mechanism can be obtained automatically without any assumptions being made in advance. The observed mode of failure and velocity diagram at collapse of an anchor block is shown in Figure 4.13 and Figure 4.14 respectively. In general, it was found that failure could be characterized by the development of a small active failure zone immediately behind the anchor, and an extensive passive failure zone in front of the anchor as depicted in

Figure 4.13 (a) and (b). It was also found that upward movement of soil wedge is accompanied by lateral deformation extending out from the anchor edge (Figure 4.13 (b) and Figure 4.14). As the anchor is pulled horizontally, the material in front of the anchor tends to lock up as it attempts to dilate during deformation. As a consequence, to accommodate the rigid soil wedge movement, the observed plastic zone is forced to extend a large distance laterally outwards into the soil mass. This soil locking phenomenon was noticed by (Rowe, 1978) who found that soil dilatancy had a significant effect on the observed plastic region at failure, which in turn resulted in substantial variations in the predicted anchor break-out factor. The condition of soil above the anchor block is very uncertain. Two small non-plastic zones were observed to develop above the anchor block as shown in Figure 4.13 (a).
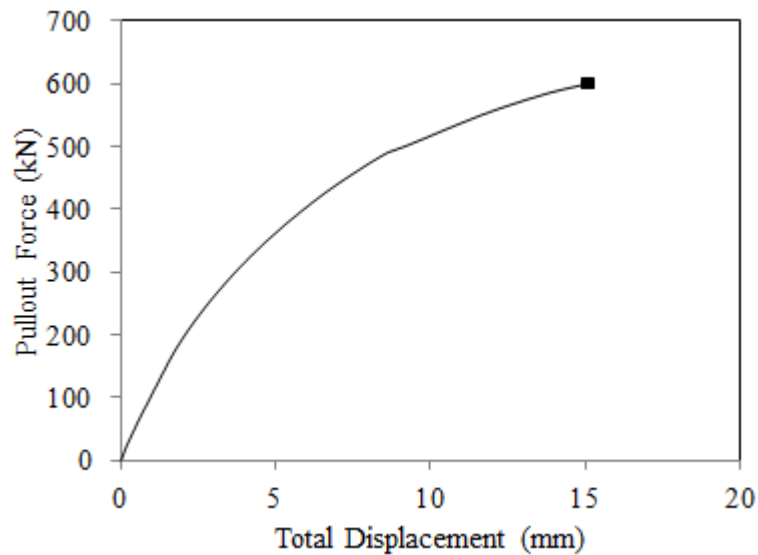
Figure 4.15 Load-displacement curves as predicted by PLAXIS for the experimental studies by Duncan and Mokwa (2001)

4.6   Remarks on Mohr-Coulomb Model

The experimental studies conducted by Duncan and Mokwa (2001), Naser (2006) and Mostofa (2013) were simulated using Mohr-Coulomb (MC) model in PLAXIS. The pullout capacity of anchor block is determined from load-displacement curve as shown in Figure 4.15, Figure 4.16 and Figure 4.17, and presented in Table 4.5 along with anchor and soil parameters used for experimental studies. From Table 4.5 it is seen that, the predicted results from MC model overestimates the test results by 16 to 47 %. This is probably due to the fact that MC model is an elastic perfectly-plastic model. It cannot simulate non-linear and inelastic behaviour of soil properly. In this case, the failure points for pullout capacity

were obtained at the end of linear portion of load-displacement curves, whereas the experimental studies by Neely et al. (1973) showed that the same state of soil is achieved at lower stress level. Hereby, the soil behaves stiffer than in reality and the numerical results obtained from the MC model are usually higher than the experimental results. The PLAXIS 3D results of Nimityongskul (2010), obtained with the soil model MC model, also overestimated the stiffness of the load displacement curve, while he studied the effects of soil slope on lateral capacity of piles in cohesive soils.
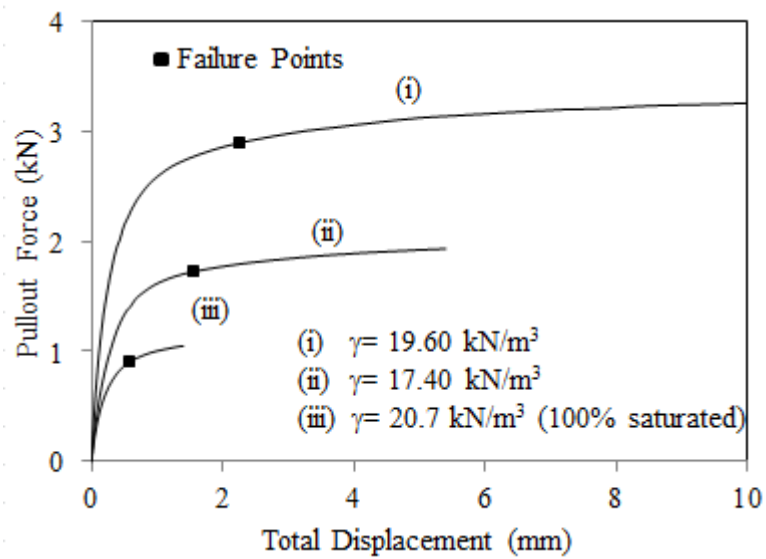
Figure 4.16 Load-displacement curves as predicted by PLAXIS for the experimental studies by Naser (2006)
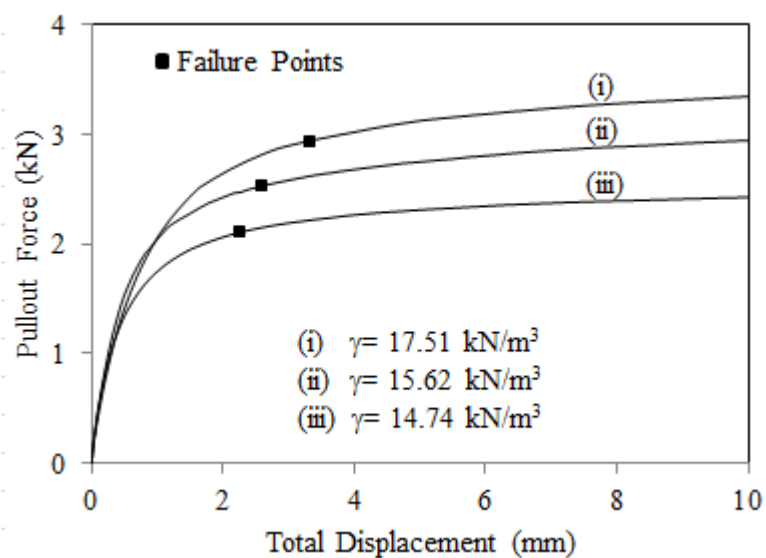
Figure 4.17 Load-displacement curves as predicted by PLAXIS for the experimental studies by Mostofa (2013)

55

Table 4.5 Anchor and soil parameters for experimental studies

Author	H (mm)	t (mm)	B (mm)	L (mm)	φ (deg.)	γ (kN/m^3)	Pullout Capacity (kN)		
							Exp.	FE-MC	% error
Duncan and Mokwa (2001)	1100	900	1100	1900	50.0	21.20	410	602	47
Naser (2006)	300	150	150	150	43.5	17.40	1.3	1.7	31
	300	150	150	150	43.5	19.60	2.3	2.9	26
	300	150	150	150	43.5	20.7[1]	0.7	0.9	29
Mostofa (2013)	475	75	150	150	37.2	14.74	1.9	2.2	16
	475	75	150	150	43.9	15.62	2.1	2.6	24
	475	75	150	150	44.8	17.51	2.3	3.0	30

[1]Saturated unit weight

In spite of this limitation, MC model was adopted in this study, since it is computationally very efficient and requires only five basic input parameters (Young's modulus, E; Poisson's ratio, v; cohesion, c; friction angle, φ; and dilatancy angle, ψ). Moreover, all the useful findings of this numerical study were made on the shape of the curves, which were plotted using non-dimensional parameters (Figure 4.7, Figure 4.10 and Figure 4.12). Thus, the qualitative trends of the curves were more important than the quantitative value of pullout capacity for this study.

CHAPTER 5
CONCLUSIONS AND RECOMMENDATIONS

5.1 General

This chapter summarizes the major findings through this study. The main objective of this study was theoretical and numerical analyses of pullout capacity of anchor block embedded in cohesionless soil. The effect of ground water table on anchor capacity was also studied and can be considered during design. The numerical analyses were conducted using Mohr-Coulomb constitutive model in PLAXIS. Of course, this research work could not capture all the field problems regarding anchor block design. However, it is expected that this research will make an important contribution to the design of anchored retaining earth wall in cohesionless soil used as backfill.

5.2 Conclusions

The following conclusions can be drawn from the results presented in this research work:

(i)   The proposed theoretical method, Eq. (3.8) and Eq. (3.10) as presented below, can be used to determine the pullout capacity of an anchor block embedded in cohesionless soil. Equation (3.8) was first formulated considering all possible contributing forces in the anchor block and wedge. Subsequently, it was simplified as Eq. (3.10) neglecting the comparatively less influencing parameters- forces acting at the side of the wedge, frictional resistance between concrete and soil and active thrust on block intended for ease. The effect of ground water table can be considered only when the water table is located at ground surface. The use of submerged unit weight (γ') instead of bulk unit weight of soil (γ) in the analytical expression is sufficient to account the effect of water table.

$$P_u = 2F_{sf}\sin\beta\,\cos\alpha - 2F_{sn}\sin\alpha + \frac{(W + 2F_{sf}\cos\beta)}{\tan\,(\beta - \,')} - P_a + F_b + F_s + F_t \quad (3.8)$$

$$P_u = \frac{W}{\tan(\beta - \,')} \quad (3.10)$$

(ii)   Equation (3.10) is facilitated with charts for quick estimation of the pullout resistance of anchor block for most frequently used shapes, cube shaped and square shaped with half of height/length of block as thickness. It is observed from those charts that the theoretical break out factor, N varies linearly with the embedment depth ratio (H/B) for a given value of angle of internal friction of soil (φ).

(iii)   The results obtained from the experimental studies in the literature were compared with the predictions from the proposed method and existing methods. The comparisons between the proposed method and experimental results appear to be better than other methods for varied condition of soil. The Mean Absolute Percentage Error (MAPE) was found to be smaller, 14.3% and 16.5% for Eq. (3.8) and Eq. (3.10) respectively, than other methods considered in this study.

(iv)   The proposed theoretical method shows very close agreement with FE analysis for embedment depth ratio, $H/B \leq 5$. However, it underestimates the break-out factors significantly for greater embedment ratio ($H/B > 5$) and, predicts nearly half as FE analysis result for H/B=9. Thus, it is recommended that the proposed theoritical method should be used for shallow depth only i.e. H/B should be less than or equal to 5.

(v)   From FE analysis, it was found that the ground water table may not have essentially any influence on pullout resistance of anchor block when it is located at or below the base of the block. However, the effect of ground water table should be considered, when the water table is anywhere between the ground surface and the base of the anchor block. In such cases, a correction factor may be calculated from Eq. (4.1) as shown below, and should be multiplied with the pullout capacity determined from the proposed theoretical method.

$$P_{u,GWT}/P_{u,dry} = -0.6\,(z/H)^2 + 1.1(z/H) + 0.5 \qquad (4.1)$$

(vi)   The size and shape of the anchor has also considerable influence on ultimate pullout resistance of an anchor block. FE analysis shows that the effect of shape is considerable for aspect ratio, $L/B \leq 2$ and is of insignificant importance for $L/B \geq 5$. As the aspect ratio increases, the influence of boundary conditions decreases, and

plain strain results (2D analysis) will be more applicable for large aspect ratios. Hence, the rectangular anchor block with $L/B \geq 5$ should be treated as strip anchor block.

(vii) Mohr-Coulomb model was found to overestimate the experimental results considerably. Despite of this limitation, Mohr-Coulomb model was adopted in this study, since all the findings were made on the shape of the curves, which were plotted using non-dimensional parameters. Thus, the qualitative trends of the curves were more important than the quantitative value of pullout capacity for this study.

(viii) From FE analysis, it was found that failure could be characterized by the development of a small active failure zone immediately behind the anchor, and an extensive passive failure zone in front of the anchor. It was also found that upward movement of soil wedge is accompanied by lateral deformation extending out from the anchor edge. However, the condition of soil above the anchor block is very uncertain. Two small non-plastic zones were observed to develop above the anchor block.

5.3   Recommendations for Future Study

During the course of theoretical and numerical analyses, there was always an urge to expand the scope of the study in order to gather some more information and to achieve some better results. Moreover, as this is frequently adopted method during design and construction of retaining wall, opportunities for future researches are numerous. Some of these future research prospects are recommended below-

(i)   Although the cohesionless soil is always preferred as a backfill material in general, sometimes cohesive soil may be encountered during backfilling. In such circumstances, design of anchor block should be made on cohesive soil, which may be studied.

(ii)   Very high retaining wall may require multi-staged anchor system. The anchor in the lowest stage may be embedded at deeper depth. In that case, new theoretical approach may be developed to study the behaviour of deep anchor.

(iii)   Sometimes, the displacement corresponding to the ultimate capacity is required for

design purposes. This can be obtained from the load-displacement curves. However, the load-displacement curves obtained from Mohr-Coulomb model in this study are not reliable, since the soil behaves stiffer than in reality. Therefore, rigorous field tests may be conducted to obtain actual load-displacement curves, or advanced constitutive model like Hardening-Soil (HS) model may be adopted which is formulated in the framework of hardening plasticity.

(iv) The ultimate capacity is achieved when anchor block is kept far away from the active failure surface behind the retaining wall. On the other hand, sometimes space constraints allow the anchor block to place near failure surfaces. In such case, partial passive resistance develops in front of the anchor block that may be studied.

(v) The effect of dynamic loading (e.g. earthquake or, liquefaction) on pullout capacity of anchor block may be investigated.

Thus, it is recommended for future study to work on these areas to capture all the problems encountered in the field during the design and construction of anchor block. Finally, it is expected that the present study will be useful to all those dealing with civil engineering projects and research works on anchored retaining wall. This research will also be useful to those who are involved in the development of standards on the determination of horizontal pull out capacity of anchor block.

REFERENCES

Akinmusuru, J. O. (1978). Horizontally Loaded Vertical Plate Anchors in Sand. *Journal of the Geotechnical Engineering Division, ASCE, 104*(2), 283-286.

Basudhar, P. K., and Singh, D. N. (1994). A Generalized Procedure for Predicting Optimal Lower Bound Break-out Factors of Strip Anchors. *Géotechnique, 44*(2), 307-318.

Bowles, J. E. (1997). Sheet-pile Walls Cantilevered and Anchored. In *Foundation Analysis and Design* (5th ed., pp. 778-780). The McGraw-Hill Companies, Inc., Singapore.

BS 8006. (1995). Strengthened/Reinforced Soils and Other Fills, Section 6.6. In *British Standard* (p. 66). London.

CFEM. (2006). *Canadian Foundation Engineering Manual* (4th ed.). Richmond, BC, Canada Canadian Geotechnical Society.

Daniel, D. E., and Olson, R. E. (1982). Failure of an Anchored Bulk-Head. *Journal of Geotechnical Engineering Division, ASCE, 108*(10), 1318-1327.

Das, B. M. (1990). Vertical Plate Anchors. In *Earth Anchors* (pp. 84-134). Amsterdam, Netherlands Elsevier.

Das, B. M. (1995). *Principles of Foundation Engineering (3rd ed.).* California Books/Cole Publishing Company.

Das, B. M. (2007). Sheet Pile Walls. In *Principles of Foundation Engineering* (6th ed., pp. 452-459). Thomson Brooks/Cole, Ontario, Canada.

Das, B. M., and Seeley, G. R. (1975). Load-Displacement Relationships for Vertical Anchor Plates. *Journal of the Geotechnical Engineering Division, American Society of Civil Engineers, 101*(GT7), 711-715.

Dickin, E. A., and King, J. W. (1997). Numerical Modelling of the Load-Displacement Behaviour of Anchor Walls. *Computers and Structures, 63*(4), 849-858.

Dickin, E. A., and Leung, C. F. (1983). Centrifuge Model Tests on Vertical Anchor Plates. *Journal of Geotechnical Engineering, ASCE, 109*(12), 1503-1525.

Dickin, E. A., and Leung, C. F. (1985). Evaluation of Design Methods for Vertical Anchor Plates. *Journal of Geotechnical Engineering, ASCE, 111*(4), 500-520.

Duncan, M., and Mokwa, R. (2001). Passive Earth Pressures Theories and Test. *Journal of Geotechnical and Geoenvironmental Engineering, ASCE, 127*(4), 248-257.

Gabr, M. A., and Borden, R. H. (1990). Lateral Analysis of Piers Constructed on Slopes. *Journal*

of Geotechnical Engieering, 116(12), 1831-1850.

Ghaly, A. M. (1997). Load-Displacement Prediction for Horizontally Loaded Vertical Plates. *Journal of Geotechnical and Geoenvironmental Engineering, American Society of Civil Engineers, 10.1061/(ASCE)1090-0241(1997)1231(74)*.

Gireesha , T., and Muthukkumaran, K. (2011). Study on Soil-Structure Interface Strength Property. *International Journal of Earth Sciences and Engineering, 4*(6), 89-93.

Hanna, A. M., Das, B. M., and Foriero, A. (1988). Behaviour of Shallow Inclined Plate Anchors in Sand. (B. M. Das, Ed.) *Geotechnical Special Publication 16, ASCE*, 54-72.

Hansen, J. B. (1966). Resistance of Rectangular Anchor Slab. *Danish Geotechnical Institute, 21*, 12-13.

Hardin, B. O., and Black, W. L. (1966). Sand Stiffness Under Various Triaxial Stresses. *Journal of the Soil Mechanics and Foundations Division, 92*(2), 27-42.

Hoshiya, M., and Mandal, J. N. (1984). Some Studies of Anchor Plates in Sand. *Soils and Foundations, 24*(1), 9-16.

Hueckel, S. (1957). Model Tests on Anchoring Capacity of Vertical and Inclined Plates. *Proceeding,4th Internation Conference on Soil Mechanics and Foundation Engineering, 2*, pp. 203-206. London, England Butterworths Scientific Publications.

Hueckel, S., Kwasniewski, J., and Baran, L. (1965). Distribution of Passive Earth Pressure on the Surface of a Square Vertical Plate Embedded in Soil. *Proceeding, 6th International Conference on Soil Mechanics and Foundation Engineering*, *2*, pp. 381-385. Montreal, Canada.

Jaky , J. (1948). Pressure in silos. *2nd ICSMFE*, *1*, pp. 103-107. London.

Janbu, N. (1963). Soil Compressibility as Determined by Oedometer and Triaxial Test., *1*, pp. 19-25. Wiesbaden, Germany.

Jesmani, M., Kamalzare, M., and Nazari, M. (2013). Numerical Study of Behavior of Anchor Plates in Clayey Soils. *International Journal of Geomechanics, 13*(5), 502-513.

Jones, C. (1996). Earth Reinforcement and Soil Structures. *Thomas Telford Services Ltd, London, UK*.

Kame, G. S., Dewaikar, D. M., and Choudhury , D. (2012). Pullout Capacity of a Vertical Plate Anchor Embedded in Cohesionless Soil. *Earth Science Research, 1*(1), 27-56.

Khan, A. J., and Sikder, M. (2004). Design Basis and Economic Aspects of Different Types of Retaining Walls. *Journal of Civil Engineering, IEB, CE 32*(1), 17-34.

Kötter, F. (1903). Die Bestimmung des Drucks an gekrümmten Gleitflächen, eine Aufgabe aus

der Lehre vom. 229-233. Berlin Univ.-Bibliothek Frankfurt am Main.

Koutsabeloulis, N. C., and Griffiths, D. V. (1989). Numerical Modelling of the Trap Door Problem. *Géotechnique, 39*(1), 77-89.

Kumar, J., and Sahoo, J. P. (2012). Upper Bound Solution for Pullout Capacity of Vertical Anchors in Sand Using Finite Elements and Limit Analysis. *International Journal of Geomechanics, 12*(3), 333-337.

Lade, P. V., and Duncan, J. M. (1975). Elasto-Plastic Stress-Strain Theory for Cohesionless Soil. *Journal of Geotechnical Engineering Division, ASCE*.

Lin, C., Han, J., Bennett, C., and Parsons, R. L. (2014). Analysis of Laterally Loaded Piles in Sand Considering Scour Hole Dimensions. *Journal of Geotechnical and Geoenvironmental Engineering, ASCE, 140*(6), 1-13.

Merifield, R. S., and Sloan, S. W. (2006). The Ultimate Pullout Capacity of Anchors in Frictional Soils. *Canadian Geotechnical Journal, 43*, 852-868.

Mirzoyan. (2007). *Lateral Resistance of Piles at the Crest of Slopes in Sand.* Master's Thesis, Brigham Young University, Department of Civil and Environmental Engineering, Provo, Utah, United States.

Mostofa, M. G. (2013). *Horizontal Pullout Resistance of Concrete Anchor Blocks in Sand Backfill.* Master's Thesis, Bangldesh University of Engineering and Technology, Department of Civil Engineering, Dhaka, Bangladesh.

Murray, E. J., and Geddes, J. D. (1987). Uplift of Anchor Plates in Sand. *Journal of Geotechnical Engineering, ASCE, 113*(3), 202-215.

Murray, E. J., and Geddes, J. D. (1989). Resistance of Passive Inclined Anchors in Cohesionless Medium. *Géotechnique, 39*(3), 417-431.

Naser, A. S. (2006). Pullout Capacity of Block Anchor in Unsaturated Sand. *Unsaturated Soils 2006 (GSP 147), Proceedings of the Fourth International Conference on Unsaturated Soils.* (pp. 403-414). Arizona ASCE.

NAVFAC DM 7.02. (1986). Foundations and Earth Structures . In *Naval Facilities Engineering Command* (pp. 91-92). Alexandria, Virginia.

Neely, W. J., Stuart, J. G., and Graham, J. (1973). Failure Loads of Vertical Anchor Plates in Sand. *Journal of the Geotechnical Engineering Division, ASCE, 99*(9), 669-685.

Nimityongskul, N. (2010). *Effects of Soil Slope on Lateral Capacity of Piles in Cohesive Soils.* PhD Thesis, Department of Civil and Construction Engineering, Oregon State University, Oregon, USA.

Niroumand, H., and Kassim, A. (2010). Analytical and Numerical Study of Horizontal Anchor Plates in Cohesionless Soils. *Electronic Journal of Geotechnical Engineering, 15*(C), 281-292.

Ovesen, N. K. (1964). Passive Anchor Slabs, Calculation Methods and Model. *Danish Geotechnical Institute, 4*, 5-39.

Ovesen, N. K. (1981). Centrifuge Tests of the Uplift Capacity of Anchors. *Proceedings of the 10th International Conference on Soil Mechanics and Foundation Engineering*, *1*, pp. 717-722. Stockholm, A.A. Balkema, Rotterdam, The Netherlands, 15–18 June 1981.

Ovesen, N. K., and Stromann, H. (1972). Design Methods of Vertical Anchor Slabs in Sand. *Proceedings, Specialty Conference on Performance of Earth and Earth-Supported Structures, American Society of Civil Engineers, 2.1*, pp. 1481-1500.

Potyondy, J. G. (1961). Skin Friction between Various Soils and Construction Materials. *Géotechnique, 11*(1), 339-353.

Reese, L. C., Cox, W. R., and Koop, F. D. (1974). Analysis of Laterally Loaded Piles in Sand. *Sixth Annual Offshore Technology Conference. 2*, pp. 473-480. Houston, Texas OTC 2080.

Rowe, R. K. (1978). *Soil Structure Interaction Analysis and Its application to the Prediction of Anchor Behaviour,* PhD Thesis, University of Sydney, Department of Civil Engineering, Sydney, Australia

Rowe, R. K., and Davis, H. (1982). The Behaviour of Anchor Plates in Sand. *Géotechnique, 32*(1), 25-41.

Sakai, T., and Tanaka, T. (1998). Scale Effect of a Shallow Circular Anchor in Dense Sand. *Soils and Foundations, 38*(2), 93-99.

Samui, P., and Sitharam, T. G. (2009). Pullout Capacity of Small Ground Anchors A Relevance Vector Machine Approach. *Geomechanics and Engineering, 1*(3), 259-262.

Singh, A. I. (1967). *Soil Engineering in Theory and Practice.* New York Asia Publishing House, Inc.

Sloan, S. W. (1988). Lower Bound Limit Analysis Using Finite Elements and Linear Programming. *International Journal for Numerical and Analytical Methods in Geomechanics, 12*, 61-67.

Smith, J. E. (1962). *Deadman Anchorages in Sand.* Washington, D.C. U.S. Naval Civil Engineering Laboratory.

Song, Z. (2008). Pullout Behaviour of Suction Embedded Plate Anchors in Clay. *PhD Thesis*,

Curtin University of Technology, Department of Civil and Construction Engineering, Perth, Australia.

Sowers, G. B., and Sowers, G. F. (1973). Failures of Bulkhead and Excavation Bracing. *Civil Engineering, ASCE, 37*(1), 72-77.

Tagaya, K., Scott, R. F., and Aboshi, H. (1988). Pullout Resistance of Buried Anchor in Sand. *Soils and Foundations, 28*(3), 114-130.

Tagaya, K., Tanaka, A., and Aboshi, H. (1983). Application of Finite Element Mehod to Pullout Resistance of Buried Anchor. *Soils and Foundations, 23*(3), 91-104.

Terzaghi, K. (1948). *Soil Mechanics in Engineering Practice.* New York Wiley.

Tiwari, B., and Al-Adhadh, A. R. (2014). Influence of Relative Density on Static Soil–Structure Frictional Resistance of Dry and Saturated Sand. *Geotechnical and Geological Engineering, 32*, 411-427.

Tiwari, B., Ajmera, B., and Kaya, G. (2010). Shear Strength Reduction at Soil Structure Interaction. *GeoFlorida 2010 Advances in Analysis, Modeling and Design* (pp. 1747-1756). Orlando, Florida, United States ASCE.

Vermeer, P. A., and Sutjiadi, W. (1985). The Uplift Resistance of Shallow Embedded Anchors. *Proceedings of the 11th International Conference on Soil Mechanics and Foundation Engineering, 12–16 August, 4*, pp. 1635-1638. San Francisco.

Zhao, L., Li, L., Yang, F., and Liu, X. (2011). Joined Influences of Nonlinearity and Dilation on the Ultimate Pullout Capacity of Horizontal Shallow Plate Anchors by Energy Dissipation Method. *International Journal of Geomechanics, 11*(3), 195-201.

APPENDIX

Load-displacemnt curve obtained from PLAXIS 3D analysis:

The experimental study conducted by Naser (2006) for γ=19.6 kN/m^3 was modelled, and the output results obtained from FE analysis, i.e. displacement and ΣMstage, is presented in column 1 and 2 of the following table. In this case, the input-load in the loading phase was 5000 kN, which was large enough to cause ultimate collapse of the soil body before ΣMstage reaching to unity. The applied load level (column 4) for a particular displacemnt was calculated multiplying ΣMstage (column 2) with 5000 kN. The applied load (column 4) was plotted against displacemnt (column 3) to obtain load-displacemnt curve, which is illustrated in Figure 4.16 (i).

Displacement (m) 1	ΣMstage 2	Displacemnt (mm) 3	Applied Load (kN) 4
0	0	0	0
1.61E-05	4.55E-05	0.016072	0.227417
1.99E-05	5.42E-05	0.019874	0.270851
2.38E-05	6.26E-05	0.023804	0.313036
2.78E-05	7.04E-05	0.027797	0.352179
3.58E-05	8.54E-05	0.03578	0.426838
4.39E-05	9.95E-05	0.04386	0.497479
5.19E-05	0.000113	0.0519	0.564809
5.99E-05	0.000126	0.059867	0.628676
6.77E-05	0.000138	0.067724	0.689357
7.16E-05	0.000144	0.071602	0.718197
7.94E-05	0.000155	0.079385	0.775166
8.72E-05	0.000166	0.087165	0.83008
0.000103	0.000187	0.102678	0.933642
0.00011	0.000196	0.110283	0.978809
0.000118	0.000205	0.117877	1.023429
0.000125	0.000213	0.125486	1.067468
0.000133	0.000222	0.133112	1.109569
0.000141	0.00023	0.140728	1.149241
0.000156	0.000245	0.155944	1.227336
0.000186	0.000274	0.186301	1.367598
0.000194	0.000279	0.193665	1.394102
0.000201	0.000284	0.200963	1.419568
0.000208	0.000289	0.208294	1.445574
0.000216	0.000294	0.215688	1.472328

Displacement (m) 1	ΣMstage 2	Displacemnt (mm) 3	Applied Load (kN) 4
0.00023	0.000305	0.230499	1.525453
0.000245	0.000315	0.245288	1.574718
0.000275	0.000334	0.274802	1.671803
0.000304	0.000351	0.304455	1.757048
0.000334	0.000367	0.333925	1.836391
0.000363	0.000381	0.363234	1.905428
0.000393	0.000394	0.392658	1.968475
0.000396	0.000395	0.396293	1.972569
0.0004	0.000395	0.399886	1.976232
0.000403	0.000396	0.403452	1.980478
0.000411	0.000398	0.41057	1.990287
0.000425	0.000403	0.424848	2.012689
0.000439	0.000408	0.439359	2.039374
0.000454	0.000414	0.454149	2.06848
0.000458	0.000416	0.458196	2.077762
0.000462	0.000418	0.46229	2.087787
0.000466	0.000419	0.466339	2.097434
0.000474	0.000423	0.474266	2.114281
0.000482	0.000426	0.482066	2.128928
0.000497	0.000431	0.497425	2.153886
0.000513	0.000435	0.512745	2.177054
0.00052	0.000437	0.520292	2.185466
0.000528	0.000439	0.527741	2.193315
0.000535	0.00044	0.535191	2.201808
0.00055	0.000444	0.550114	2.219539
0.00058	0.000451	0.580157	2.257281
0.000611	0.000459	0.611049	2.296514
0.000642	0.000466	0.642163	2.331124
0.000673	0.000473	0.673313	2.364056
0.000704	0.000479	0.704485	2.393564
0.000736	0.000484	0.73561	2.420641
0.000767	0.000489	0.766669	2.445688
0.000798	0.000494	0.797668	2.469252
0.000829	0.000498	0.828622	2.491688
0.00086	0.000503	0.85956	2.512992
0.00089	0.000507	0.890492	2.532957
0.000921	0.00051	0.921416	2.551411
0.000952	0.000514	0.952302	2.568348
0.000983	0.000517	0.983104	2.583822
0.001014	0.00052	1.013816	2.59847
0.001044	0.000523	1.044469	2.612708
0.001075	0.000525	1.075103	2.626699

Displacement (m) 1	ΣMstage 2	Displacemnt (mm) 3	Applied Load (kN) 4
0.001106	0.000528	1.105725	2.640236
0.001136	0.000531	1.136347	2.653127
0.001167	0.000533	1.166977	2.665227
0.001198	0.000535	1.197618	2.676522
0.001228	0.000537	1.228299	2.687293
0.001259	0.000539	1.258964	2.697435
0.00129	0.000541	1.289578	2.70698
0.00132	0.000543	1.320147	2.716024
0.001351	0.000545	1.350681	2.72466
0.001381	0.000547	1.381185	2.732949
0.001412	0.000548	1.411667	2.740942
0.001473	0.000551	1.472557	2.756098
0.001533	0.000554	1.533378	2.77057
0.001594	0.000557	1.594139	2.784238
0.001655	0.000559	1.654849	2.797129
0.001716	0.000562	1.715521	2.809348
0.001776	0.000564	1.776147	2.821063
0.001837	0.000567	1.836794	2.832913
0.001897	0.000569	1.897438	2.844283
0.001958	0.000571	1.958071	2.855044
0.002019	0.000573	2.018682	2.865136
0.002079	0.000575	2.079264	2.874469
0.00214	0.000577	2.139806	2.883085
0.002261	0.00058	2.260864	2.900148
0.002382	0.000583	2.381842	2.915723
0.002442	0.000585	2.442293	2.923121
0.002563	0.000587	2.563044	2.936719
0.002684	0.00059	2.683691	2.950225
0.002744	0.000591	2.744113	2.957042
0.002865	0.000594	2.86483	2.970081
0.002985	0.000596	2.985386	2.982303
0.003106	0.000599	3.105838	2.994048
0.003226	0.000601	3.226038	3.005632
0.003286	0.000602	3.285986	3.01098
0.003346	0.000603	3.345955	3.015185
0.003466	0.000605	3.465866	3.023466
0.003585	0.000606	3.585439	3.031414
0.003705	0.000608	3.704785	3.040188
0.003824	0.00061	3.824006	3.049159
0.003943	0.000612	3.943081	3.058054
0.004062	0.000613	4.061923	3.066269
0.004181	0.000615	4.180519	3.074383

Displacement (m) 1	ΣMstage 2	Displacemnt (mm) 3	Applied Load (kN) 4
0.004299	0.000617	4.299338	3.082572
0.004418	0.000618	4.418256	3.09067
0.004537	0.00062	4.537251	3.098741
0.004656	0.000621	4.656353	3.106654
0.004776	0.000623	4.775514	3.114224
0.005014	0.000626	5.013556	3.128326
0.005132	0.000627	5.132227	3.133658
0.005251	0.000628	5.25081	3.138076
0.005369	0.000628	5.369392	3.141883
0.005488	0.000629	5.487982	3.145545
0.005607	0.00063	5.606579	3.149721
0.005725	0.000631	5.725085	3.154124
0.005962	0.000632	5.962004	3.162169
0.006021	0.000633	6.021176	3.164496
0.00608	0.000633	6.080362	3.1667
0.006199	0.000634	6.19881	3.171005
0.006317	0.000635	6.317316	3.175235
0.006436	0.000636	6.436127	3.17942
0.006674	0.000637	6.67392	3.187118
0.006912	0.000639	6.911743	3.194463
0.00715	0.00064	7.149528	3.201781
0.007179	0.000641	7.179271	3.202866
0.007209	0.000641	7.209008	3.203593
0.007268	0.000641	7.268468	3.204472
0.007387	0.000641	7.38738	3.205739
0.007506	0.000641	7.506348	3.20742
0.007744	0.000642	7.744401	3.21225
0.007983	0.000644	7.982516	3.218376
0.008042	0.000644	8.042221	3.221031
0.008102	0.000645	8.101986	3.223708
0.008222	0.000646	8.221503	3.228667
0.00846	0.000647	8.460103	3.235986
0.008579	0.000648	8.579121	3.238647
0.008698	0.000648	8.698012	3.240514
0.008936	0.000649	8.935729	3.243963
0.008965	0.000649	8.965482	3.244627
0.008995	0.000649	8.99526	3.245204
0.009055	0.000649	9.054829	3.246017
0.009174	0.000649	9.173949	3.247294
0.009412	0.00065	9.411933	3.250248
0.00965	0.000651	9.64962	3.254519
0.009887	0.000652	9.887186	3.260602

Displacement (m) 1	ΣMstage 2	Displacemnt (mm) 3	Applied Load (kN) 4
0.010125	0.000653	10.12451	3.26594
0.010243	0.000654	10.24301	3.268165
0.010361	0.000654	10.36146	3.270262
0.01048	0.000654	10.47994	3.27206
0.010717	0.000655	10.71692	3.275383
0.010836	0.000655	10.8356	3.277163
0.010895	0.000656	10.89506	3.277956
0.011014	0.000656	11.01394	3.279541
0.011252	0.000657	11.25157	3.282662
0.011489	0.000657	11.48892	3.285975
0.011726	0.000658	11.72604	3.289493
0.011755	0.000658	11.75544	3.290502
0.011785	0.000658	11.78479	3.291473
0.011843	0.000659	11.84349	3.292959
0.011961	0.000659	11.96091	3.295069
0.012079	0.000659	12.07866	3.295765
0.012197	0.000659	12.19671	3.296236
0.012433	0.00066	12.43347	3.29851
0.01267	0.00066	12.67026	3.301213
0.012789	0.000661	12.78853	3.302966
0.013025	0.000661	13.02503	3.306245
0.013498	0.000662	13.4978	3.31216
0.013734	0.000663	13.73401	3.315441
0.013793	0.000663	13.79294	3.316188
0.013852	0.000663	13.85182	3.316852
0.01397	0.000664	13.96951	3.31798
0.014205	0.000664	14.20481	3.320142
0.014323	0.000664	14.32278	3.321373
0.014559	0.000665	14.55887	3.32387
0.014795	0.000665	14.79498	3.326326
0.015267	0.000666	15.26692	3.331393
0.015503	0.000667	15.50272	3.333447
0.015739	0.000667	15.73866	3.336545
0.015975	0.000668	15.97462	3.339348
0.016211	0.000668	16.21063	3.340934
0.016447	0.000668	16.44667	3.341975
0.016919	0.000669	16.91857	3.344037
0.01739	0.000669	17.39029	3.346562
0.017508	0.00067	17.50836	3.348005
0.017626	0.00067	17.62648	3.349372
0.017863	0.00067	17.86257	3.351567
0.018334	0.000671	18.33412	3.354849

70

Displacement (m) 1	ΣMstage 2	Displacemnt (mm) 3	Applied Load (kN) 4
0.018569	0.000671	18.56949	3.356124
0.018687	0.000671	18.68706	3.356857
0.018922	0.000672	18.92206	3.358432
0.01904	0.000672	19.03952	3.359351
0.019274	0.000672	19.27432	3.361112
0.019392	0.000672	19.39171	3.362027
0.019626	0.000673	19.62645	3.363791
0.019744	0.000673	19.74384	3.364584
0.019979	0.000673	19.97862	3.366104
0.020213	0.000674	20.21333	3.367593
0.020331	0.000674	20.3307	3.368339
0.020565	0.000674	20.56541	3.369746
0.0208	0.000674	20.80005	3.371114
0.021035	0.000675	21.0346	3.372515
0.021152	0.000675	21.15186	3.373349
0.021386	0.000675	21.38635	3.375029
0.021621	0.000675	21.62078	3.376584
0.02209	0.000676	22.08951	3.379606
0.022558	0.000677	22.55792	3.382556
0.022675	0.000677	22.67509	3.383296
0.022792	0.000677	22.79233	3.383869
0.023027	0.000677	23.02677	3.384932
0.023495	0.000677	23.49538	3.387398
0.023612	0.000678	23.61216	3.388229
0.023729	0.000678	23.72889	3.389097
0.023846	0.000678	23.84556	3.389907
0.024079	0.000678	24.07882	3.391469
0.024195	0.000678	24.19536	3.39203
0.024312	0.000679	24.31191	3.392503
0.024428	0.000679	24.42845	3.392924
0.024661	0.000679	24.66148	3.393782
0.024894	0.000679	24.89443	3.394761
0.025127	0.000679	25.12732	3.395825
0.025593	0.00068	25.59296	3.398006
0.025709	0.00068	25.70924	3.398568
0.025826	0.00068	25.82552	3.399156
0.026058	0.00068	26.05805	3.40033
0.026523	0.000681	26.52296	3.402671
0.027452	0.000681	27.4521	3.40744
0.027916	0.000682	27.91616	3.409786
0.028032	0.000682	28.03209	3.41024
0.028148	0.000682	28.14799	3.410639

Displacement (m) 1	ΣMstage 2	Displacemnt (mm) 3	Applied Load (kN) 4
0.02838	0.000682	28.37975	3.411401
0.028843	0.000683	28.84313	3.412958
0.029306	0.000683	29.30629	3.414745
0.029538	0.000683	29.53785	3.416046
0.030001	0.000684	30.00083	3.418561
0.030926	0.000685	30.92628	3.423283
0.031389	0.000685	31.38862	3.425138
0.031851	0.000685	31.85076	3.426512
0.032775	0.000686	32.77465	3.429287
0.033698	0.000686	33.69808	3.432304
0.033756	0.000687	33.7557	3.432857
0.033813	0.000687	33.81331	3.433263
0.033928	0.000687	33.92849	3.433948
0.034159	0.000687	34.1588	3.435177
0.034389	0.000687	34.38903	3.436203
0.034619	0.000687	34.61931	3.437212
0.03508	0.000688	35.07994	3.439182
0.03531	0.000688	35.31037	3.440119
0.035771	0.000688	35.77122	3.441757
0.036002	0.000688	36.00156	3.44224
0.036462	0.000689	36.46219	3.443177
0.036923	0.000689	36.92261	3.444269
0.037383	0.000689	37.38279	3.445669
0.037613	0.000689	37.61276	3.446549
0.038073	0.00069	38.07251	3.448349
0.038532	0.00069	38.53203	3.450068
0.038991	0.00069	38.9913	3.451862
0.03945	0.000691	39.45028	3.453857
0.039909	0.000691	39.90918	3.455803
0.040827	0.000692	40.82676	3.459517
0.041285	0.000692	41.28537	3.461322
0.041515	0.000692	41.51457	3.462127
0.041973	0.000693	41.97281	3.463377
0.042431	0.000693	42.43098	3.464573
0.04266	0.000693	42.65989	3.465207
0.043118	0.000693	43.11768	3.466312
0.044033	0.000694	44.03332	3.46846
0.044949	0.000694	44.94933	3.470837
0.045408	0.000694	45.40761	3.472249
0.045637	0.000695	45.63684	3.473069
0.045866	0.000695	45.86614	3.473874
0.046325	0.000695	46.32489	3.47525

Displacement (m) 1	ΣMstage 2	Displacemnt (mm) 3	Applied Load (kN) 4
0.047243	0.000696	47.24268	3.477677
0.048161	0.000696	48.16061	3.480033
0.04862	0.000696	48.6196	3.481153
0.049079	0.000696	49.07864	3.48215
0.049538	0.000697	49.53774	3.482985
0.050456	0.000697	50.456	3.48457
0.051374	0.000697	51.37429	3.486133
0.051833	0.000697	51.83334	3.487127
0.052063	0.000698	52.06281	3.487677
0.052522	0.000698	52.52177	3.488657
0.05344	0.000698	53.43975	3.490365
0.054358	0.000698	54.35759	3.492043
0.055275	0.000699	55.27518	3.494008
0.055734	0.000699	55.73383	3.495085
0.056651	0.000699	56.651	3.497172
0.05688	0.0007	56.88023	3.497706
0.057339	0.0007	57.33867	3.498667
0.057797	0.0007	57.79713	3.499515
0.058256	0.0007	58.25558	3.500307
0.058485	0.0007	58.4848	3.500687
0.058599	0.0007	58.59941	3.500841
0.058829	0.0007	58.82863	3.501093
0.059287	0.0007	59.28708	3.501582
0.059746	0.0007	59.74554	3.502152
0.060204	0.000701	60.20399	3.502756
0.060662	0.000701	60.66243	3.503413
0.061121	0.000701	61.12084	3.50415
0.061579	0.000701	61.57921	3.504947
0.062038	0.000701	62.03756	3.505779
0.062496	0.000701	62.49588	3.506628
0.062954	0.000701	62.95418	3.507463
0.063412	0.000702	63.41246	3.508266
0.063871	0.000702	63.87072	3.509032
0.064787	0.000702	64.78718	3.510466
0.065245	0.000702	65.24536	3.511129
0.065704	0.000702	65.70352	3.511719
0.06662	0.000703	66.61981	3.512796
0.067078	0.000703	67.0779	3.513359
0.067536	0.000703	67.53598	3.513911
0.067994	0.000703	67.99403	3.514447
0.068452	0.000703	68.45206	3.51498
0.06891	0.000703	68.91006	3.515523

Displacement (m) 1	ΣMstage 2	Displacemnt (mm) 3	Applied Load (kN) 4
0.069368	0.000703	69.36802	3.516086
0.069826	0.000703	69.82594	3.516674
0.070284	0.000703	70.28383	3.517278
0.070742	0.000704	70.74168	3.517885
0.071199	0.000704	71.19949	3.518485
0.071657	0.000704	71.65728	3.519087
0.072115	0.000704	72.11503	3.51969
0.07303	0.000704	73.03047	3.520894
0.073946	0.000704	73.94582	3.522088
0.074861	0.000705	74.8611	3.523262
0.075776	0.000705	75.77625	3.524363
0.076234	0.000705	76.23381	3.52486
0.076691	0.000705	76.69137	3.525268